

POTENTIAL ACOUSTIC BENEFITS OF CIRCULATION CONTROL ROTORS

Robert M. Williams

David W. Taylor Naval Ship Research and Development Center

Ian C. Cheeseman

University of Southampton

SUMMARY

The Circulation Control Rotor (CCR) possesses certain unique aerodynamic characteristics which may alter the fundamental aeroacoustic mechanisms responsible for noise generation on a rotating blade. The purpose of this research, in the absence of directly applicable experimental data for the CCR, is to theoretically examine the various potential source mechanisms and attempt to predict their contribution to the overall rotor sound pressure level. Results from a new theory for airfoil trailing edge noise are presented. Modifications and extensions to other source theories are described where it is necessary to account for unique aspects of CC aerodynamics. The CCR, as embodied on an X-Wing vertical take off and landing (VTOL) aircraft, is used as an example for computational purposes, although many of the theoretical results presented are generally applicable to other CC applications (such as low speed rotors, propellers, compressors, and fixed wing aircraft). Using the analytical models, it is shown that the utilization of CC aerodynamics theoretically makes possible unprecedented advances in rotor noise reduction. For the X-Wing VTOL these reductions appear to be feasible without incurring significant attendant performance and weight penalties.

INTRODUCTION

Circulation Control Rotors (CCR) have been undergoing more or less continuous research since the early 1960's (refs. 1 to 4). This technology has now matured to the point where two U.S. Navy advanced development rotor programs are reaching the full scale wind tunnel evaluation stage. The first of these developments is a relatively low speed CCR intended to demonstrate a remarkable simplification of the helicopter rotor hub. A 13.4 m (44 ft) diameter, 4 bladed rotor is currently undergoing whirl testing by Kaman Aerospace preparatory to entry in the NASA Ames 12 x 24 m (40 x 80 ft) tunnel and eventual flight testing on the UH-2 airframe. A secondary objective of the program will be to investigate the potential of the CCR to reduce vibratory airloads both by active means (higher harmonic blowing) and by using the inherent passive characteristics of CC airfoils wherein the lift is substantially independent of velocity. The basic CCR concept employed in the Kaman program is illustrated schematically in figure 1. Briefly, a thin jet sheet of air is ejected tangentially over the rounded trailing edge of a quasi-elliptical airfoil, suppressing boundary layer separation and moving the rear stagnation streamline toward the lower surface, thereby increasing lift in proportion to the duct pressure. The azimuthal variation of lift is controlled by a simple nondynamic pneumatic valve in the hub.

For higher speeds and advance ratios, a second duct and leading edge slot are used (fig. 2) so that the rotor can develop significant lift in the region of reverse flow. Two-dimensional airfoil experiments showed that it is possible to develop large lift coefficients by blowing from either slot individually *or from both simultaneously*. The latter technique is used for advance ratios greater than 0.5 where the retreating blade experiences "mixed flow" (i.e., locally reversed flow on the inboard sections and forward flow on the outer sections). This is the CCR implementation used in

the X-Wing, a unique stoppable rotor VTOL concept. A 7.62 m (25 ft) diameter X-Wing rotor is currently being fabricated by the Lockheed California Company for testing late in 1978.

The X-Wing potentially represents a major breakthrough in subsonic VTOL design and has eventual applicability to a wide range of military and civil missions. Although the focus of current interest is on resolution of certain critical proof-of-concept technologies, it is, nevertheless, of interest to explore the design aspects of a civil version (which might look similar to the artist's conception in fig. 3). It was previously known that the X-Wing should possess several outstanding civil VTOL design features such as excellent range/payload, high 'block speed' and relative insensitivity to gusts. The effect of noise constraints on the design, however, were totally unknown—hence the reason for the present study. That acoustic design requirements can be extremely important in rotary VTOL design is evidenced by several civil application studies. For example, reference 5 indicates an increment in gross weight of approximately 25 percent to achieve a noise reduction of 10 PNdB on a tilt rotor VTOL design. It is reasonable to suspect therefore that in the highly competitive civil transport market the margin for economic viability may well hinge on the impact of noise requirements on the aircraft design.

In the absence of any applicable measurements, the acoustic characteristics of the CCR (and in particular an X-Wing CCR) are essentially unknown at present. The only acoustic test ever performed on a CCR was conducted at the National Gas Turbine Establishment (NGTE), U.K. on a very different design to that of the X-Wing. The rotor, an early prototype of I.C. Cheeseman's original CCR, was 3.7 m (12 ft) in diameter and utilized a circular airfoil section. Despite its relative crude design this rotor was found to produce virtually no rotational noise and approximately 5 dB reduction of broadband noise relative to a conventional rotor.

A direct application of current semiempirical theories indicates that the CCR should readily achieve large noise reductions by simply reducing tip speed. In the case of the X-Wing this is an attractive possibility because the rotor is *designed* for operation at all rpm's (resonances excluded). Furthermore, the blowing system and blade planform are designed by the high speed 'conversion' maneuver from rotary to fixed wing flight. This latter characteristic suggests that it may be possible to utilize the excess blowing power available in hover and at low speed to enable the rotor to operate at reduced tip speeds. These low tip speed possibilities appeared sufficiently promising that it was decided to investigate the acoustics of the CCR in greater detail. In particular, the need to either revise conventional theories or to develop new ones to account for the unique aerodynamic mechanisms of a CCR was quite apparent. As the research progressed, a very intriguing possibility appeared: due to the unique fluid mechanics of a low velocity boundary layer control wall jet operating over the curved Coanda surface and controlling the circulation, the aeroacoustic mechanisms were themselves unique. In fact, according to theory, a properly designed CCR will possess *major noise reductions relative to conventional rotors at identical operating conditions*. No less than *five* of the ten separate source mechanisms identified were found (theoretically) to be substantially reduced by the aeroacoustic characteristics of the CCR.

SYMBOLS

AR	aspect ratio
B	number of rotor blades
b/c	wake width-to-chord ratio
C_{d_p}	profile drag coefficient
C_{d_w}	'wake drag' coefficient

C_ℓ	lift coefficient
C_p	pressure coefficient
C_T	thrust coefficient
C_μ	jet momentum coefficient
c	chord length, m (ft)
D	rotor diameter (slot span), m
D/t	slot span-to-height ratio
f_p	peak SPL frequency
$f_{p\ell}$	'5 dB down' lower frequency
f_{pu}	'5 dB down' upper frequency
h	height, m
L/D_e	lift to equivalent drag ratio
M	Mach number
R	distance to microphone from source, m
R_N	Reynolds number
S	wing area (or rotor disk area), m^2
T/S	disk loading
t/c	slot height-to-chord ratio
V	velocity, m/s
X	dimensionless rotor radius
Z/c	downstream distance from trailing edge-to-chord ratio
α	angle of attack, deg.
γ	turbulence intensity
δ_w/c	wake vertical deflection-to-chord ratio
θ	microphone elevation with respect to rotor plane, positive downward, deg.
λ	planform taper ratio C_{tip}/C_{root} (or turbulence wave length)
σ	solidity ratio

Abbreviation

rpm revolutions per minute

POTENTIAL BROADBAND NOISE SOURCES

The possible significant sources of so-called 'broadband' noise radiation from a CCR may be categorized as follows (refer to fig. 4):

- (1) Classical 'trailing edge noise' (sometimes called 'vortex noise') associated with the turbulent interaction of the viscous shed wake (made up of the jet and boundary layers) and the rigid airfoil trailing edge.
 - (2) 'Laminar boundary layer instability noise' produced by an aeroacoustic feedback between viscous trailing wake pressure disturbances (apparently due to wake transition) and the instability point of the lower surface laminar boundary layer.
 - (3) 'Jet noise,' actually comprising several separate mechanisms: (a) free jet 'mixing noise' (in the case of a wake velocity excess); (b) free jet 'excess noise' produced by the interaction of the free jet turbulence with the rigid airfoil trailing edge; and (c) 'wall jet noise' produced by turbulent mixing and surface pressure fluctuations on the curved Coanda surface itself.
 - (4) 'Incident turbulence noise' produced primarily by the airfoil unsteady response to the normal component of the inflow turbulence (this source may also exhibit discrete noise spectra).
 - (5) Direct radiation from the separating surface boundary layer.
- These source mechanisms are associated with the two-dimensional airfoil section. In addition, there is a potentially important three-dimensional 'tip radiation noise' which is:
- (6) Produced by separated flow and high turbulence in the boundary layer region of the rotor tip.

POTENTIAL DISCRETE FREQUENCY NOISE SOURCES

The potential sources of 'discrete' or 'rotational' noise for the CCR appear to be essentially identical to conventional rotors as follows:

- (7) 'Gutin' type noise due to the rotation of the blade steady forces.
- (8) Noise associated with periodic variation of the blade forces due to variations of inflow angle and blade cyclic lift control.
- (9) Under certain conditions where close vortex-blade interactions occur (such as steep descent and low shaft angles) additional impulsive blade pressure fluctuations are produced due to sudden changes of inflow angle, giving rise to blade 'bang.'
- (10) As advancing tip Mach number increases the blade profile geometry (thickness distribution and chord) gives rise to combined monopole-dipole-quadrupole contributions which produce impulsive 'slap' noise.

BROADBAND NOISE REDUCTION WITH CC

(1) **Trailing edge noise** - A new theory of trailing edge noise has been developed which allows the calculation of both conventional rotors and circulation control rotors.* The theory indicates that the maximum sound intensity varies directly with the product of drag coefficient squared, velocity to the fifth power, and wake-based Strouhal number; and varies inversely with the

*Presentation of the trailing edge noise theory will be made in a future paper due to space limitations.

dimensionless wake width. Figure 5 presents a comparison of this new theory for aircraft power-off fly over data from reference 6. Figure 6 presents a comparison of 'peak broadband excrescence noise' data as defined by Wright (ref. 7) and the trailing edge theory modified to include the effect of a source near the rotating rotor tip. It can be surmised that the theory is accurate, devoid of empiricism, and applicable to arbitrary airfoil, wing, or rotor configurations. To apply the theory to the CCR it is necessary to utilize two-dimensional airfoil data from tests of the applicable CC airfoil. Figure 7 shows measured variations of the trailing wake width and wake drag coefficients for the X-Wing tip section (as required by the theory). Figure 8 presents the calculated noise reduction boundaries based on this two-dimensional data (relative to the noise of a 'baseline' conventional NACA 0012 airfoil of equal chord at zero angle of attack). It can be noted that a relatively wide design corridor of lift coefficient and angle of attack is predicted wherein the *inherent* X-Wing trailing edge noise will be significantly lower than for a conventional rotor. (These curves are based only on the drag coefficient and wake width and do not reflect the additional reductions which accrue due to reduced tip speed and tip chord.) A measure of caution is needed when applying these two-dimensional test results to an actual rotor blade such as the X-Wing. The existence of obstructions upstream of the slot (such as air holes in the main spar) will produce some spanwise variation of the Coanda sheets. These 'shadows' induce three-dimensional effects which may modify the two-dimensional mechanism described.

(2) Laminar boundary layer instability noise - The presence of discrete acoustic tones has been detected in airfoil tests and glider fly over data. Tam (ref. 8) and Wright (ref. 7) have apparently separately identified the source of these tones as a result of a lower surface laminar boundary layer instability participating in an aeroacoustic feedback loop with the airfoil wake. Using the stability theory, the presence of this acoustic source has been identified on a CC lifting cylinder operating at very high lift coefficients. These calculations are directly applicable to the experimental data on the 3.7 m (12 ft) CC rotor tested by the NGTE (which employed circular sections). Figure 9 presents the calculated instability center frequencies for the experimental rotor hover data. These results suggest that the instability mechanism was, in fact, the *dominant* noise source for this (very quiet) low tip speed circular section CCR. Using a similar approach, the boundary layer stability of the X-Wing root and tip sections was calculated for a high-lift hover condition. Figure 10 presents calculations for several different rotor sizes and indicates that *the X-Wing should be entirely free* of this acoustic source. It should be noted, however, that these results are calculated for a small positive blade pitch setting such that the tip section is operating at zero angle of attack. At higher angles of attack or much lower tip speeds the lower surface boundary layer will tend toward full laminar flow.

(3) Jet Noise - The phenomena of CC jet noise was analyzed using a semi-empirical method developed from turbulent wall jet acoustic theory and limited experimental data from the NGTE (circular section) 3.7 m (12 ft) CCR measured with the rotor stopped. This data represents an extreme case because the Coanda wall jet actually curves 180 degrees around the airfoil section and then separates into quiescent surroundings, thus introducing wall jet, free jet mixing, and some trailing edge or slot edge noise as well as any 'upstream' noise due to turbulence from the internal air valving in the rotor head. Figure 11 presents the measured rotor jet noise in terms of the wall jet theory parameters. Two different observation angles, measured with respect to the rotor tip path plane, are included. The variation with jet Mach number can be seen to be quite different from conventional free jet theory at the low jet Mach numbers and varies not unlike the 'excess noise' of subsonic jet engines in this regime. Using the power law exponent variations derived from these data, the predicted jet noise and peak SPL frequency for the X-Wing are shown in figure 12. In view of the fact that relative velocity effects are known to have a significant noise reduction effect, it is concluded that the jet noise should be quite low over the high subsonic slot exit velocity range of the X-Wing. This conclusion is also in agreement with subjective assessments made during the NGTE tests, DTNSRDC CCR model rotor tests and tests of the Tip Air Mass

Injection System (TAMI) at NASA Langley. A note of caution is needed here, however. The large variation of the velocity exponent at low jet velocities suggests that there are at least two distinct phenomena which dominate the 'jet noise.' At high jet velocities the V_{jet}^8 follows the expected trend and indeed appears to be jet mixing noise. At lower velocities the data suggests another source mechanism, quite possibly due to separated flow upstream of the jet exit. In this circumstance the 'jet noise' at low jet velocities would be strongly design dependent and would be sensitive to the details of the valving system and, in particular, to any separated flow close to the jet exit itself. The latter case is potentially of concern for the X-Wing flight demonstrator design where significant turbulence is introduced by air holes cut in the main spar.

(4) Incident Turbulence Noise - The most difficult noise source to calculate on the CCR is that due to variations of the inflow velocity over the disk. The resultant noise may contain both broadband and (if blade-to-blade correlation exists) also discrete components. The origins of the inflow variation on a rotor have been attributed to a variety of factors including blade twist, atmospheric turbulence, recirculation, tip vortex oscillations, etc. However, in a close examination of the rotor broadband mechanisms of a large variety of rotors, propellers, and fans under widely varying conditions, Wright (ref. 7) has reached the rather startling finding that these explanations do not adequately or consistently account for the arbitrary variations found in practice. Wright concluded that the incident turbulence (or 'excess broadband') noise mechanism is more likely "...intrinsically connected with the rotor, (and) appears to be supercritical on the slightest flow asymmetry."

One rather compelling argument in support of Wright's conclusion can be based on the unique experimental data of Schieman (ref. 9). Schieman's measurements of the noise of an untwisted rotor in hover and of a nonlifting, twisted rotor in axial flow strongly suggest that the viscous wake has a very marked effect. Figure 13 shows typical data from these tests. Reductions of as much as 15 dB in the comparative spectra were demonstrated when the (viscous) wake was 'blown' downstream by axial tunnel flow. The incident turbulence theory of Fink (ref. 10) has been modified to produce the correlation with Schieman's data shown in figure 14 (for a rotor operating in its own wake) where the independent parameters are the inflow turbulence intensity and turbulence wave length. A maximum turbulence intensity value of 16 percent was found to predict the maximum SPL. In view of the fact that typical normal turbulence levels in the free shear layer behind an airfoil can be on the order of 15 to 20 percent it seems quite plausible that the 'intrinsic' mechanism alluded to by Wright is actually a blade interaction with the viscous shed wake behind a preceding blade. It is possible that these wakes 'stack up' on each other, layer upon layer, with a separation dependent on the downwash velocity through the disk. Any slight perturbation of the layer would then result in a small change of circulation on the following blade due to the redistribution of the inplane velocity normal to a given span station (the blade element is essentially experiencing stratified flow). A change of circulation produces a shed wake which further perturbs the viscous layer (and so forth) until a system of 'standing waves' is set up around the azimuth.

Based on the preceding theoretical correlation, a calculation of the incident turbulence noise can be attempted for the CCR. Using measured airfoil data and corrections for three-dimensional effects, the wake deflection and turbulence intensity encountered by the following blade was estimated as shown in figure 15. The turbulence encountered by the following blade is assumed to vary directly with the drag coefficient (from mixing length theory for a free wake) and inversely with the wake deflection (lift). It can be noted from these calculations that for values of section lift coefficient greater than 0.5 the incident turbulence noise due to self-induced wake phenomena would be negligible.

The validity of the preceding explanation of incident turbulence noise has yet to be fully confirmed despite the encouraging correlation of figure 14. Certainly the apparent absence of

incident turbulence noise from the high lift NGTE CCR data is encouraging. However, the basic incident turbulence acoustic mechanism is heavily dependent on the rate of change of surface pressure with incidence, particularly close to the leading edge. The circular sections of this rotor exhibit very low gradients ($dC_p/d\alpha$), hence the final conclusion is not obvious. In any event, the possibility of other incident turbulence sources cannot yet be discounted for the CCR as embodied on the X-Wing. In the absence of other solutions, the use of reduced tip speeds may be required to finally suppress this noise.

(5-6) Direct boundary layer noise and 'tip radiation noise' - Direct radiation from the attached turbulent boundary layers has been shown by several investigators to be about two orders of magnitude below other broadband sources. However, if separated flow exists, the levels of fluctuating surface pressure may be as much as 30 dB higher than for the attached case. The regions where separation may occur on a CCR are (a) just beneath the separating wall jet and (b) at the rotor tip. The former case is apparently the same phenomena as the trailing edge noise discussed previously. This can be deduced from cross correlations on conventional airfoils of the normal component of turbulence and the pressure in the separated zone at the trailing edge. (The physical problem is actually one of sound refraction about the edge from the turbulent quadrupole source.) The situation at the rotor tip is rather unclear at present. However, there is sufficient experimental information available to definitely relate tip drag to noise level. The emerging picture of the phenomena is quite complex. The high velocity air sweeping up around the rotor tip entrains the lower surface boundary layer and encounters a retarding pressure gradient along the highly curved tip surface. The (entrained) boundary layer separates under these conditions giving rise to a separation locus in the streamwise direction, on the rotor tip proper. The separated flow then sweeps up and over and forms a reattachment line inboard of the tip (similar to a delta wing vortex). The separating viscous fluid forms the well known 'vortex core' with a considerably higher velocity defect and turbulence level than the inboard airfoils. It is quite possible that this turbulence interaction with the blade tip and trailing edge is the dominant broadband noise mechanism of the tip - not unlike the trailing edge noise mechanism discussed previously. (Other source mechanisms may also be present; for example, Cheeseman has noted that the vortex location fluctuates more with 'noiser' tips, apparently giving rise to increased rotational noise.)

The approach taken to reduce this noise mechanism for the X-Wing tip was to develop a design which, in concept, essentially eliminated it. Such a design (shown in fig. 16) is a simple rotation of the Coanda surface about the tip airfoil midchord. The Coanda jet then extends around the tip, blowing in the spanwise direction. Tuft and oil measurements of this design (tested as a wing tip) indicate that: (a) the tip region with tip blowing 'off' was partially separated, but with blowing 'on' was observed to be fully attached; (b) the tip vortex actually formed off of the tip, approximately in the plane of the blade (as shown in fig. 17); and (c) that the measured drag was significantly reduced at high lift (fig. 18). The overall aerodynamic efficiency (measured as a fixed wing equivalent lift to drag ratio, L/D_e) did not increase however, due to the additional blowing power required. The conclusion drawn from this work is that the potential high frequency broadband source of the rotor tip should be essentially eliminated by the Coanda tip design.

DISCRETE FREQUENCY (ROTATIONAL) NOISE REDUCTION WITH CC

(7-8) 'Gutin' noise and blade load variation - The Lowson-Ollerhead theory (ref. 11) for predicting the noise due to both steady and unsteady blade loads is directly applicable to the CCR. The primary uncertainty in this theory is the determination of the proper harmonic order and magnitude for the blade lift force. Several studies have indicated the need for inclusion of additional loading harmonics - depending on the blade twist. (In general, an increase in blade twist

produces a more uniform downwash distribution with fewer wake distortions.) For the X-Wing, the hover downwash distribution can be 'designed' to be very close to ideal by choice of either collective pitch setting, and/or slot height distribution. Figure 19 illustrates this point by showing the predicted downwash variation for the X-Wing at various collective pitch settings with a simple linear slot height distribution. This design feature, in conjunction with the 'velocity independence' aspect of a CC airfoil and a more uniform chordwise loading profile, should permit the X-Wing to enjoy the more rapid fall-off in loading harmonics given by the unmodified theory. Figure 20 presents the predicted rotational noise for the X-Wing in hover at various tip speeds (a case applicable to low speed forward flight is also shown).

(9) Vortex-blade interaction noise - The potential of the CCR for reducing impulsive 'bang' noise is largely unknown at present; however, the application of available theory suggests that the rotor may not produce this source at all. According to Leverton's theoretical and experimental analysis of blade 'bang' (ref. 12), the sound pressure level is given by

$$\text{SPL}_n = 10 \log_{10} [V^4 A_n^2 (r_0 - r_1)^2] + \text{constant}$$

where, V is the velocity of the blade passing through the vortex, A_n is the amplitude of the n th harmonic of the blade upwash velocity, and $(r_0 - r_1)$ is the span width over which the gust acts. One major noise reduction effect with the CCR is the intersection velocity produced by operation at lower tip speeds (higher C_T/σ). In the case of the X-Wing with Coanda tip blowing, the peak vortex core tangential velocities are expected to be reduced due to the increased mixing produced by the jet. Wake vorticity measurements by Rochester Applied Science (ref. 13) on a similar normal blowing tip design (fig. 21) indicated a reduction of the peak core velocities of more than 50 percent, a doubling of the core radius and an outboard shift of the vortex position. The latter effect (shown in fig. 17) was measured with the Coanda tip installed on a fixed X-Wing blade. Furthermore, model rotor acoustic testing of the tip air mass axial injection system (ref. 14) showed marked reductions of blade 'bang' intensity (fig. 22). The axial system is believed to produce less efficient mixing and peak velocity reductions than the present Coanda design. Application of the Leverton equation using the measured velocity profiles and a rotor tip speed of 167 m/s (550 ft/sec) indicates that the X-Wing blade vortex noise will be below the subjectively significant level.

(10) Blade Slap - Operations in a flight condition where blade slap may be produced is not anticipated for X-Wing (except possibly for a short duration near conversion speeds). The various source mechanisms associated with high speed impulsive noise, or blade slap, are currently undergoing intensive study. Research by Schmitz (ref. 15) and others indicated the primary factors to be: (a) advancing tip Mach number; (b) blade thickness, thickness distribution, and chord near the rotor tip (chord appears to be the dominant term); (c) blade drag; and (d) the existence of shock waves. In the case of the X-Wing with generally low tip speeds, the primary effect of advancing tip Mach number will be reduced (except close to the speed for conversion to a stopped mode). Furthermore, although the section thickness ratio is high at the tip (15 percent for an X-Wing CCR relative to 6-10 percent for a conventional rotor), the blades incorporate a 2:1 planform taper so that the *dimensional* thickness and chord are actually somewhat reduced. For example, assuming an X-Wing CCR and a conventional rotor of the same diameter, number of blades, and solidity (but with much lower tip speeds, for example 152 m/s (500 ft/sec) for CCR and 213 m/s (700 ft/sec) for the 10 percent thick conventional rotor), the CCR would have equal thickness but only 2/3 the chord dimension.

In the case of the blade drag (c) the lower chord and generally lower advancing tip speeds appear to more than offset the somewhat higher drag coefficients found on the advancing side of the X-Wing. The transonic behavior of a CC airfoil operating near zero angle of attack and zero lift is determined by the off-setting effects of high thickness ratio and the near optimum elliptical

thickness distribution. As a consequence the 15 percent ellipse has a critical Mach number of 0.75 compared with approximately 0.78 for a 10 percent symmetrical airfoil. It can therefore be seen that even the shock phenomena would appear to be reduced when accounting for the smaller blade chord.

PERFORMANCE AND WEIGHT PENALTIES

The X-Wing is a unique VTOL concept which can potentially extend the application of rotorcraft into several different areas where noise is an important factor. The apparent favorable modification of fundamental acoustic mechanisms may actually produce a quieter rotor at the nominal 204 m/s (670 ft/sec) 'baseline' X-Wing CCR design tip speed. It may also be desirable, however, to fully exploit the variable rpm capability and excess hover 'blowing' capacity of this rotor. It is useful, therefore, to perform a preliminary assessment of the design penalties which are incurred by operation at reduced tip speeds and higher blowing levels.

Figures 23 and 24 present the calculated variations of hover power components of a 15.2 m (50 ft) diameter X-Wing. Constant rotor thrust is prescribed so that, with the rotor geometry specified, only the collective pitch and blowing level are varied with tip speed to tradeoff shaft 'torque' power and blowing power. An antitorque fan was designed for the 'baseline' configuration of the study and perturbed slightly for other designs. It can be noted from the trends that total power is relatively insensitive to a large range of tip speeds - a sharp contrast with conventional rotors. Another interesting aspect is the variation of rotor shaft torque. As tip speed is reduced the increased blowing allows the 'torque' power (profile, pumping and induced power) to also reduce so that the torque itself varies only weakly with rpm.

A general conclusion which may be deduced from the preceding example is that a CC rotor of X-Wing planform can perform efficiently at low tip speeds without the necessity to increase blade chord. For tip speeds in the range of 167 m/s (550 ft/sec) essentially *no power penalty* is incurred relative to the 204 m/s (670 ft/sec) 'baseline' design tip speed. The actual shaft power is reduced so that in a propulsion system design which provides the blowing air from an independent source (such as fan bypass air) the engine shaft power and size would actually be slightly *reduced* by about 5 percent. The increased blowing power requirement of almost 50 percent is the price paid for reduced tip speed with no rotor geometry change and only a small (6 percent) increase of torque. However, for the X-Wing the blowing power is inconsequential in view of the excess installed to perform the conversion maneuver.

The design weight penalty to operate at lower rotor tip speed is not amenable to simple treatment for the X-Wing. The rotor geometry and blowing power are actually designed by forward flight (conversion) requirements so that it is necessary to conduct a complete design study to assess the overall impact. The propulsion system selection is also inextricably involved in such a study because of the sharing of torque power and blowing power. Figure 25 illustrates one of several possible schemes for providing rotor torque, blowing air, and propulsive power. The figure depicts variable pitch fans providing power at high rpm directly to a centrifugal compressor and then into a main gear box. This arrangement permits extraction of the blowing power on the high rpm side of the transmission thus significantly reducing the maximum transmission torque requirement. A further advantage of this propulsion system is the quieting potential of the variable pitch propulsion fan which may either be operated at low pitch settings or decoupled entirely.

An indication of the weight trend associated with reducing tip speed for this particular propulsion system is shown in figure 26. For the present example no additional rotor system weight or compressor weight is introduced by low rpm operations as these components are both

designed by the conversion flight condition. In effect, only the drive system and tail fan weights are impacted by the low rpm requirements.

These results are very encouraging in that they imply a net weight penalty of only about 0.5 percent to drop tip speed from the baseline 204 m/s (670 ft/sec) to 167 m/s (550 ft/sec) for low rotor noise. However, they do not encompass the additional weight penalties which would be incurred in *quieting the tail fan*. The 'baseline' tail fan is unacceptably noisy and would require a 30-40 percent reduction in tip speed and a large increase in diameter to achieve compatible PNdB levels with the main rotor. The proper calculation of this penalty is complex and beyond the scope of this paper. It is worthwhile mentioning, however, that a large diameter antitorque tail fan is not the only means possible to produce large moments, low weight, and low noise. An interesting alternate approach is to incorporate circulation control on the aft fuselage itself as sketched in figure 27. The fuselage would operate in downwash velocities on the order of 18 m/s (60 ft/sec) and with a thick elliptical cross section it could easily generate lift coefficients of 5.0 or more in an extremely efficient manner. A rough calculation for the civil X-Wing design indicates that a very efficient antitorque system would be possible. The CC fuselage blowing will not be a replacement for a tail fan (or internal fan), which is required for certain flight conditions where the main rotor wake is skewed off of the fuselage. However, during hover and low speed flight it should significantly unload the primary controller thus producing a lower weight, lower power solution to the antitorque noise problem. It is significant to note that first mention of this concept was made in one of the earliest landmark analyses of helicopter noise by Davidson and Hargest in 1965 (ref. 1). More recently (1978) Logan (ref. 16) has actually implemented the concept with considerable success in the OH-6A light helicopter.

CONCLUSIONS AND RECOMMENDATIONS

The present theoretical study focused on the fundamental aeroacoustic mechanisms of the Circulation Control Rotor. There appears to be an excellent inherent potential with the CCR for making major advances in the reduction of rotorcraft noise without incurring significant performance and weight penalties. The single outstanding source requiring further definition is the incident turbulence noise. If, as suggested herein, the dominant contributor to incidence fluctuations is the wake of the preceding blade, then the problem is amenable to direct control by CC. In this case the entire noise spectrum would be suppressed down to the (very low) trailing edge and jet noise levels without recourse to reduced tip speeds. If however, there are other more significant causes (for example, atmospheric turbulence) then it will be necessary to reduce tip speed. Quite apparently, the next logical step is to conduct a careful acoustic experiment to both resolve this key issue and also to explore the other theoretical claims.

With regard to the overall X-Wing civil concept, the antitorque system requires further definition. In particular, fuselage-mounted Coanda blowing, the fan-in-fuselage, and circulation control incorporated on the antitorque fan itself all appear worthy of further consideration.

REFERENCES

1. Davidson, J. M.; and Hargest, T. G.: Helicopter Noise, Jol. of the Royal Aeronautical Society, vol. 69, May 1965, pp. 325-336.
2. Cheeseman, I. C.: The Application of Circulation Control by Blowing to Helicopter Rotors, Jol. of the Royal Aeronautical Society, vol. 71, no. 679, July 1967.
3. Williams, R. M.: The Application of Circulation Control to a Stopped Rotor Aircraft, vol. 1, no. 1, VERTICA, Pergamon Press, 1976.
4. Stone, M. B.; and Englar, R. J.: Circulation Control - A Bibliography of NSRDC Research and Selected Outside References, Naval Ship Research and Development Center Report 4108, Jan. 1974.
5. Gibs, J.; Stepniewski, W. Z.; and Spencer, R.: Effects of Noise Reduction on Characteristics of a Tilt-Rotor Aircraft, Jol. of Aircraft, vol. 13, no. 11, Nov. 1976, pp. 919-925.
6. Fink, M. R.: Approximate Prediction of Airframe Noise, Jol. of Aircraft, vol. 13, no. 11, Nov. 1976, pp. 833-834.
7. Wright, S. E.: The Acoustic Spectrum of Axial Flow Machines, Institute of Sound and Vibration Research, University of Southampton, Rep. 69, Apr. 1975.
8. Tam, C. K. W.: Discrete Tones of Isolated Airfoils, Jol. of the Acoustical Society of America, vol. 55, no. 6, June 1974, pp. 1173-1177.
9. Schieman, J.; et al: Rotating-Blade Vortex Noise, Mideast Region Symposium on Status of Testing and Modeling Techniques for V/STOL Aircraft, Essington, Pa., Oct. 1972.
10. Fink, M. R.; Schlinker, R. H.; and Amiet, R. K.: Prediction of Rotating-Blade Vortex Noise from Noise of Nonrotating Blades, NASA CR-2611, Mar. 1976.
11. Lowson, M. V.; and Ollerhead, J. B.: A Theoretical Study of Helicopter Rotor Noise, Jol. of Sound and Vibration, vol. 9, Mar. 1969, pp. 197-222.
12. Leverton, J. W.: Helicopter Noise - Blade Slap, (Part 1: Review and Theoretical Study), NASA CR-1221, Oct. 1968.
13. Shipman, K. W.; White, R. P.; and Balcerak, J. C.: Drag Reduction of a Lifting Surface by Alteration of the Forming Tip Vortex, Rochester Applied Science Associates, Rep. 74-06, May 1974.
14. White, R. P.: Wind Tunnel Tests of a Two Bladed Model Rotor to Evaluate the TAMI System in Descending Forward Flight, Systems Research Laboratories, Inc., SRL Rep. 14-76-2, 1976.
15. Schmitz, F. H.; and Yung, H. Yu: Theoretical Modeling of High-Speed Helicopter Impulsive Noise, Third European Rotorcraft and Powered Lift Aircraft Forum, Aix-En-Provence, France, Sept. 1977.
16. Logan, A. H.: Evaluation of a Circulation Control Tail Boom for Yaw Control, USARTL-TR-78-10, Mar. 1978.

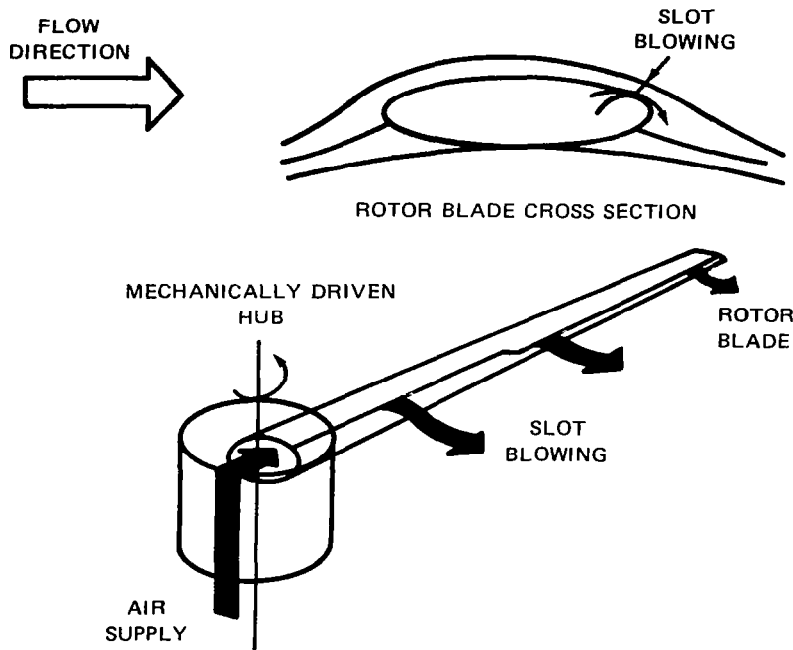


Figure 1.- Circulation Control Rotor - basic concept.

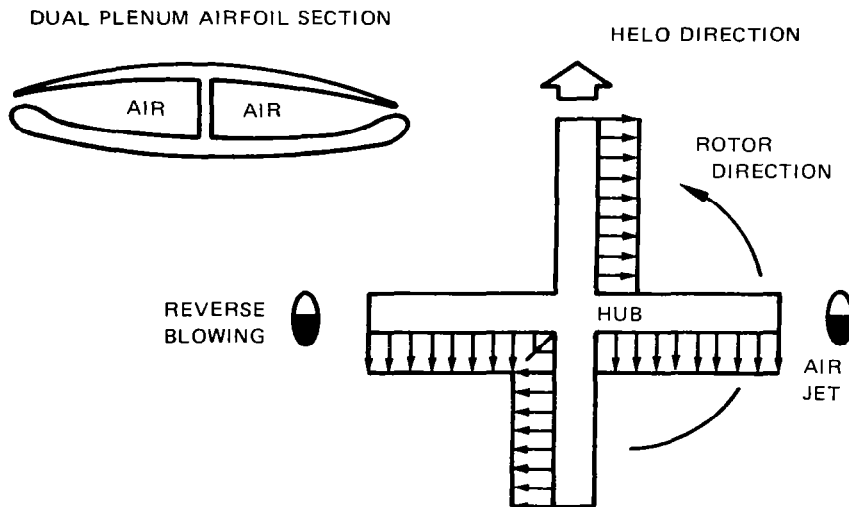


Figure 2.- Dual blowing concept for operation at high advance ratios and during conversion of the X-Wing.

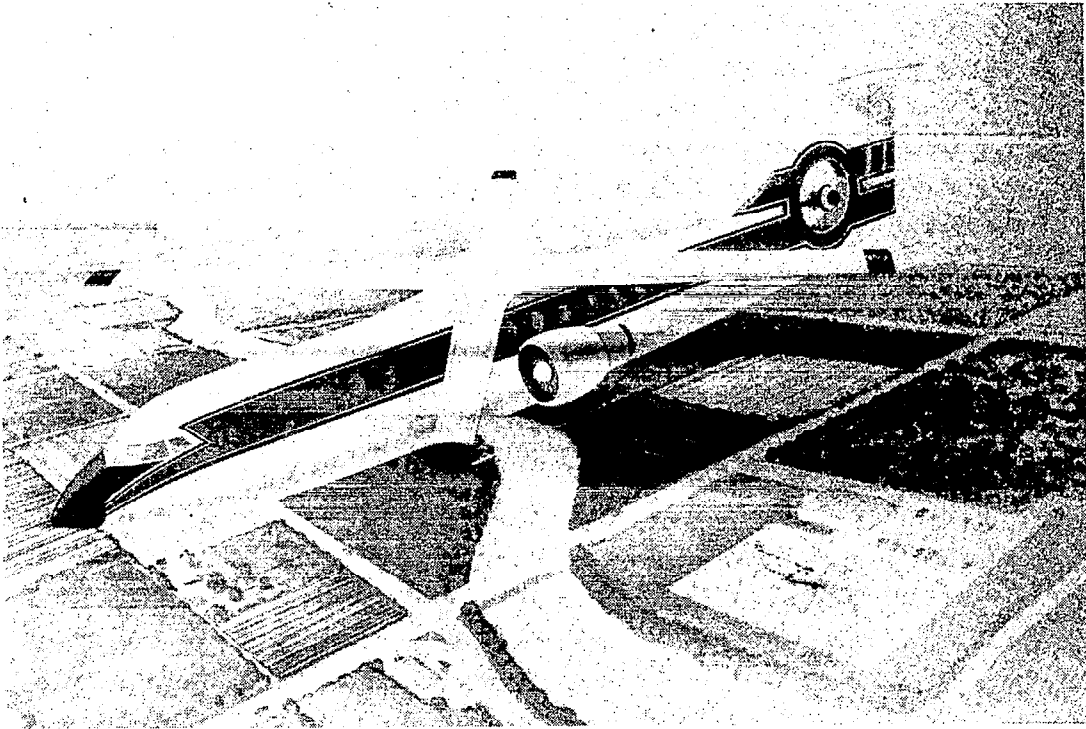


Figure 3.- Conceptual X-Wing civil transport.

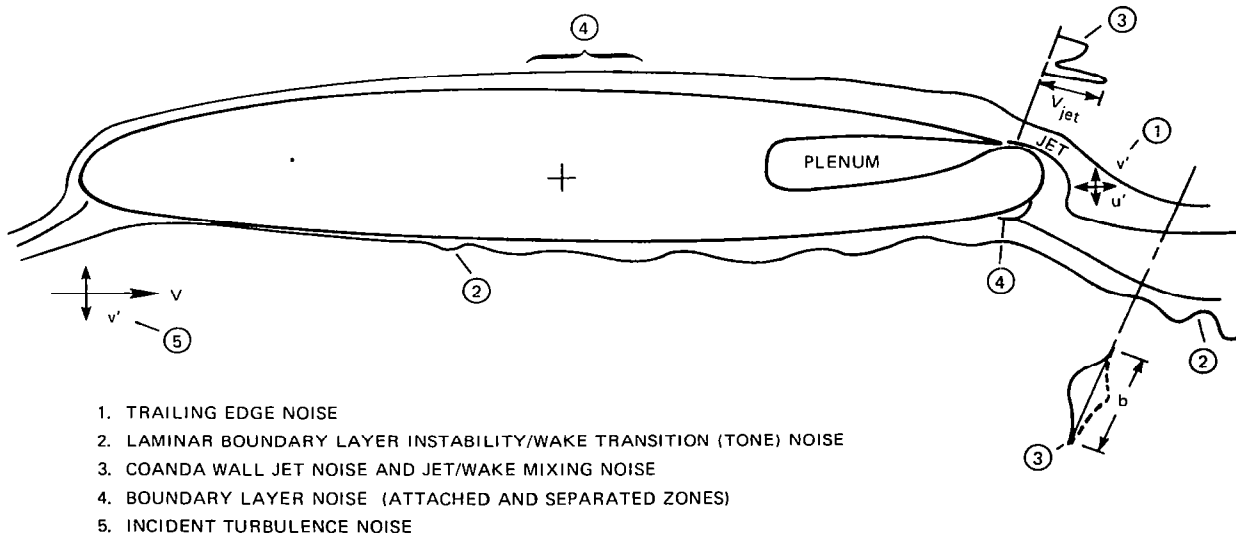
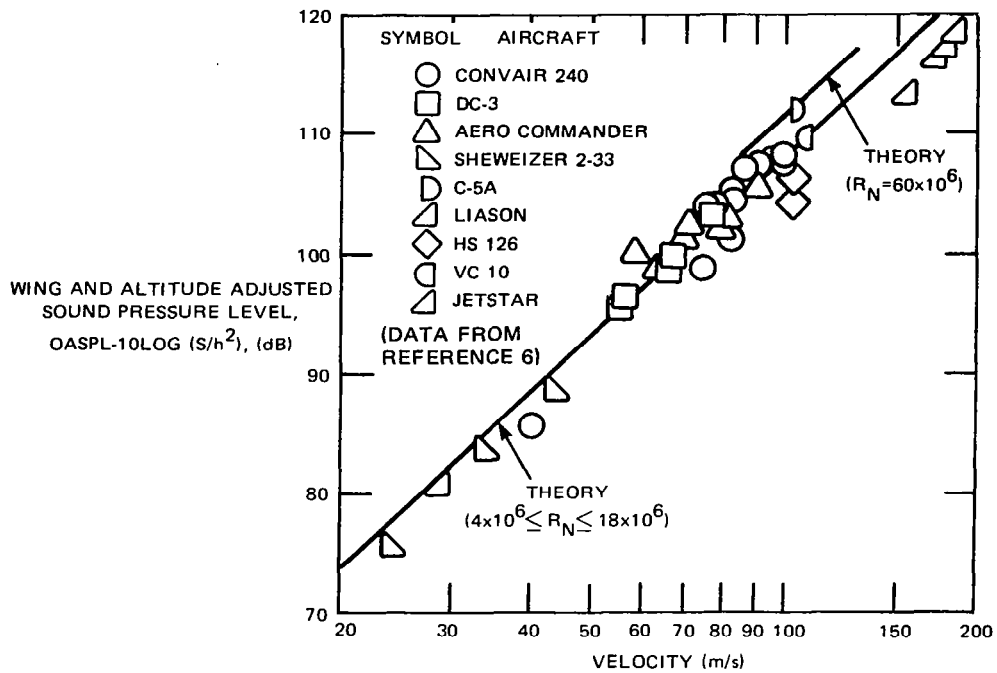
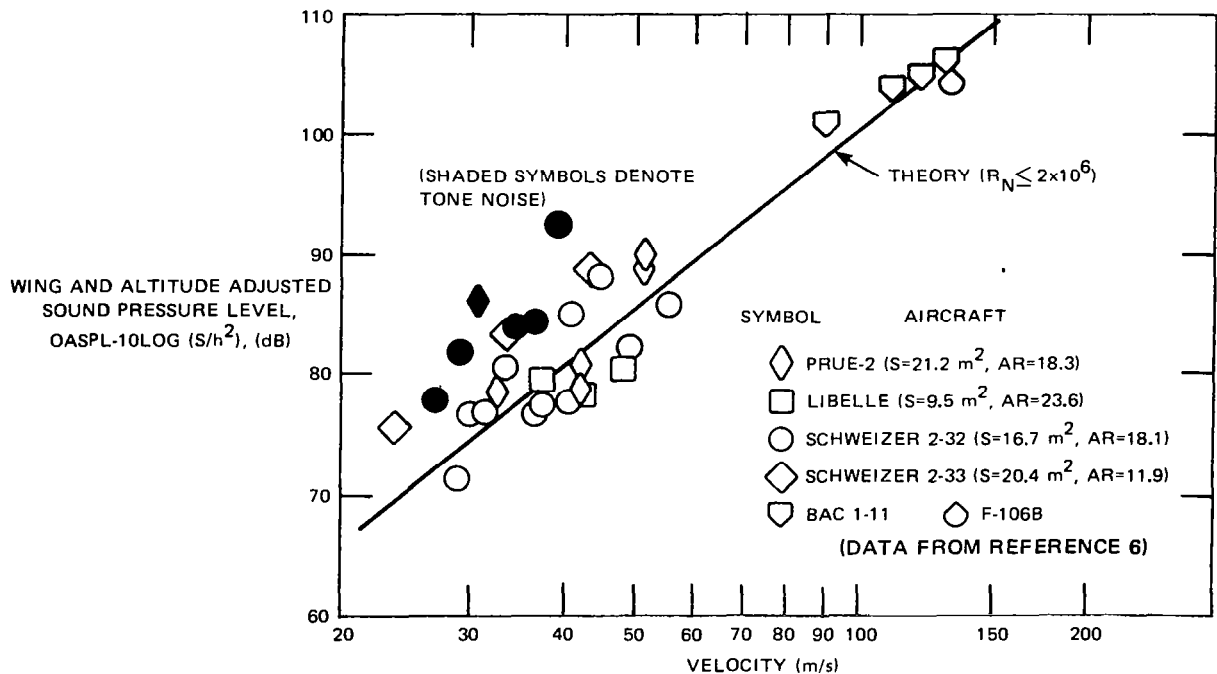


Figure 4.- Potential broadband noise mechanisms of a Circulation Control airfoil.



(a) Measured and calculated OASPL for conventional airframes with retracted gear and flaps.



(b) Measured and calculated OASPL for low drag aircraft (primarily gliders).

Figure 5.- Comparison of new trailing edge noise theory with fly-over data.

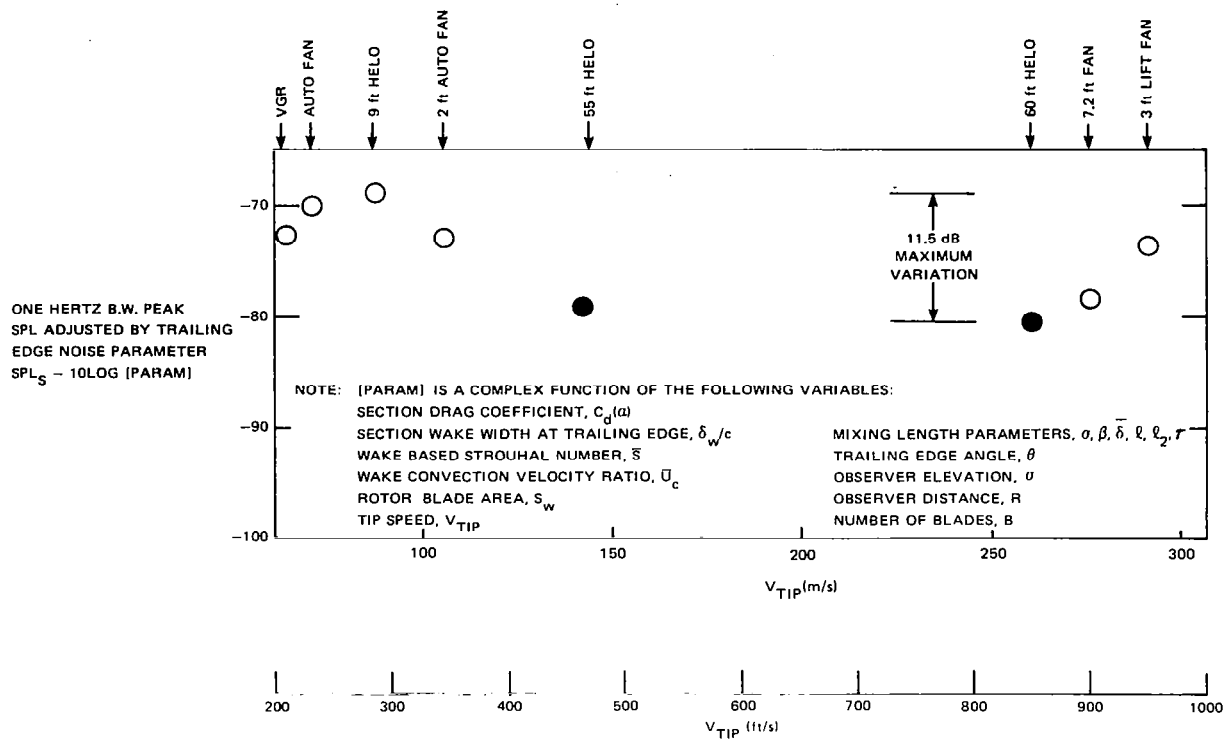


Figure 6.- Evaluation of new trailing edge noise theory using the peak broad-band excrescence data of Wright (ref. 7). (1 ft = 0.3048 m.)

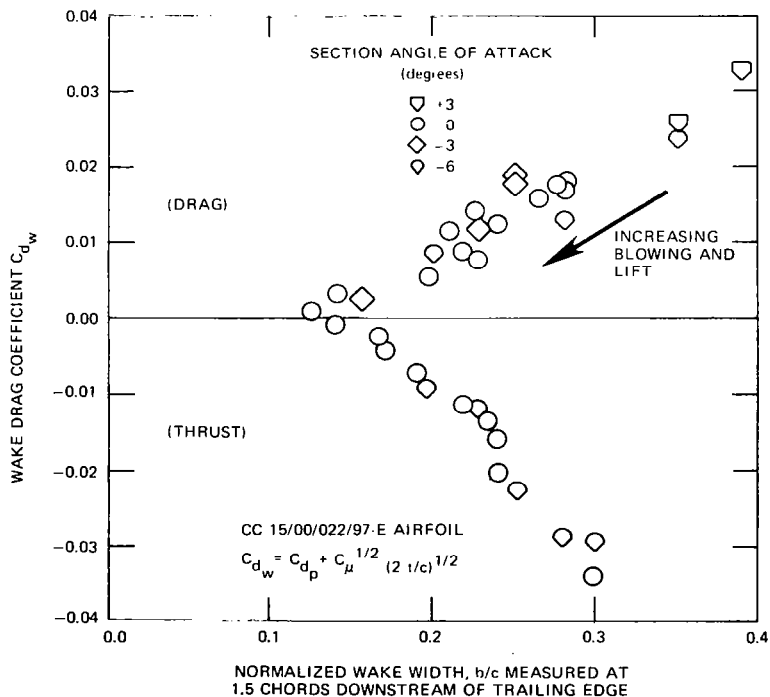


Figure 7.- Measured variation of the viscous wake width of the X-Wing tip section with wake drag coefficient.

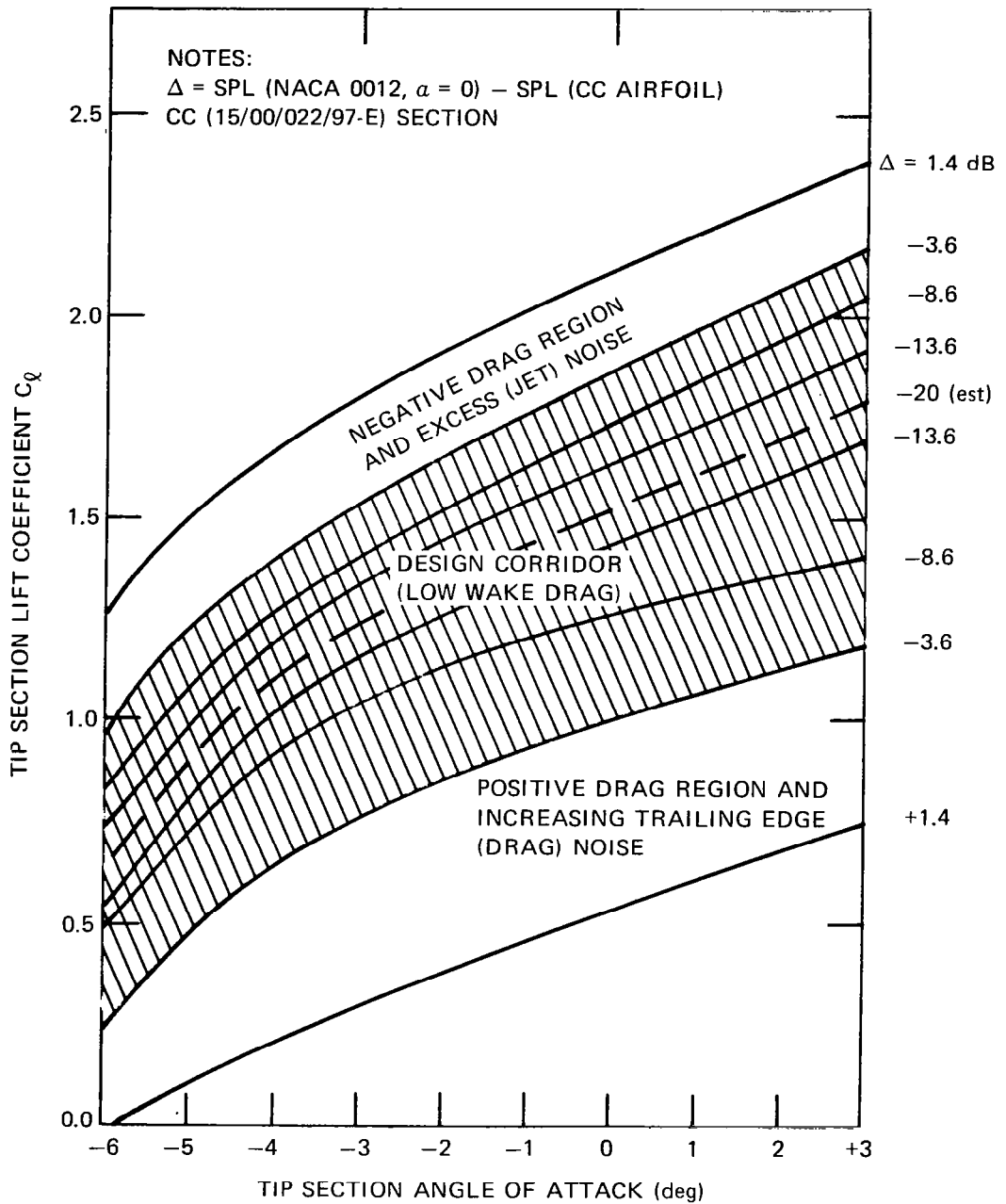
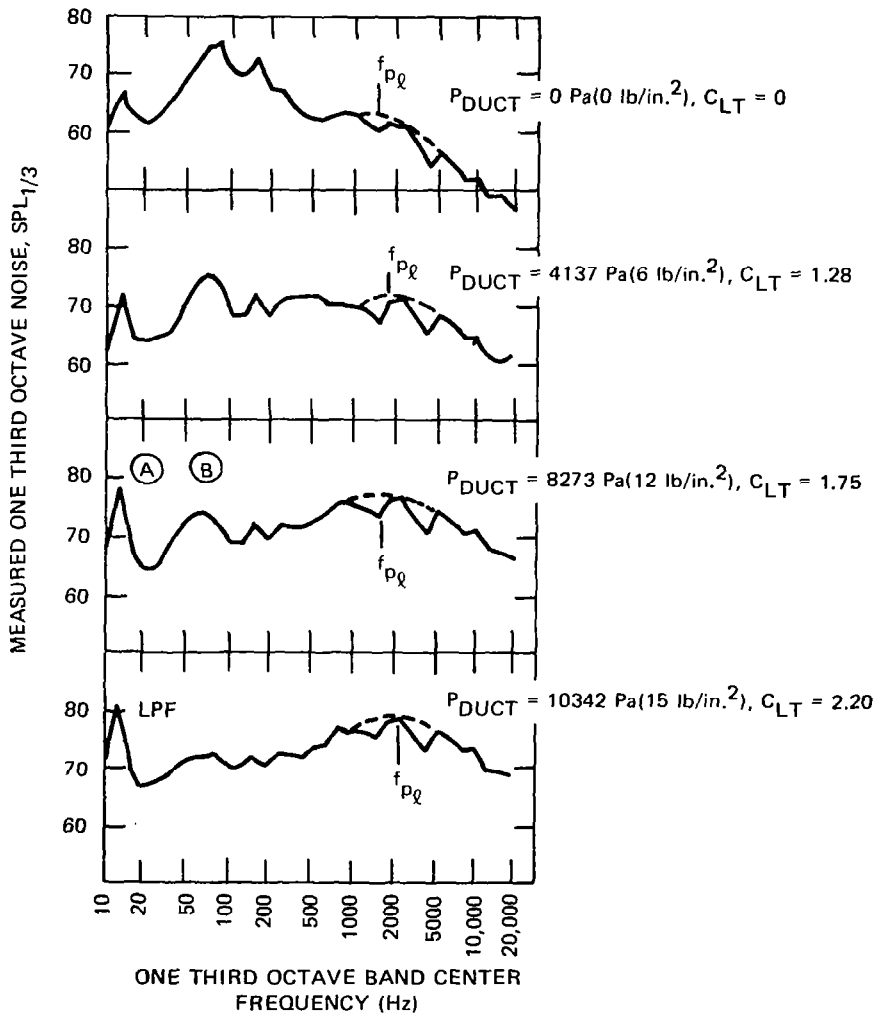
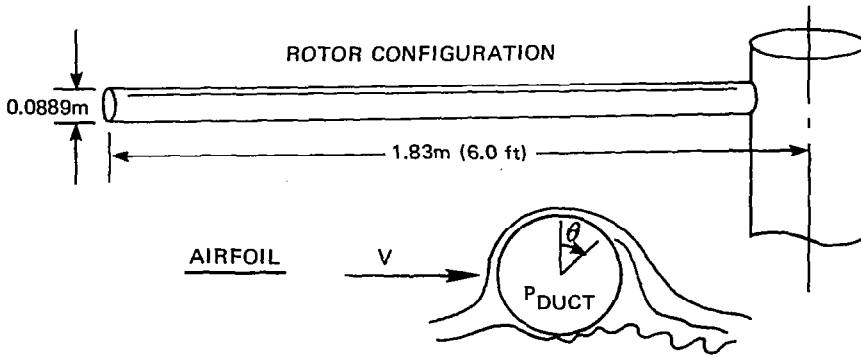


Figure 8.- Predicted trailing edge noise reduction of the X-Wing tip section relative to a NACA 0012. (Reference airfoil at zero angle of attack and lift.)



NOTES:

$f_{p\ell}$ IS THE MINIMUM ALLOWABLE FREQUENCY FOR TOLLMEIN-SCHLICHTING WAVES TO OCCUR AT SOME POINT ON THE BLADE

2 BLADES

$V_{TIP} = 78.3 \text{ m/s (257 ft/s)}$

$C_{LT} = 2(C_T/\sigma)$

RADIUS/DIA = 3.0

ELEVATION, $\theta = 45 \text{ deg}$

Figure 9.- Comparison of experimental data with stability theory for the 3.66 m (12 foot) NGTE CCR.

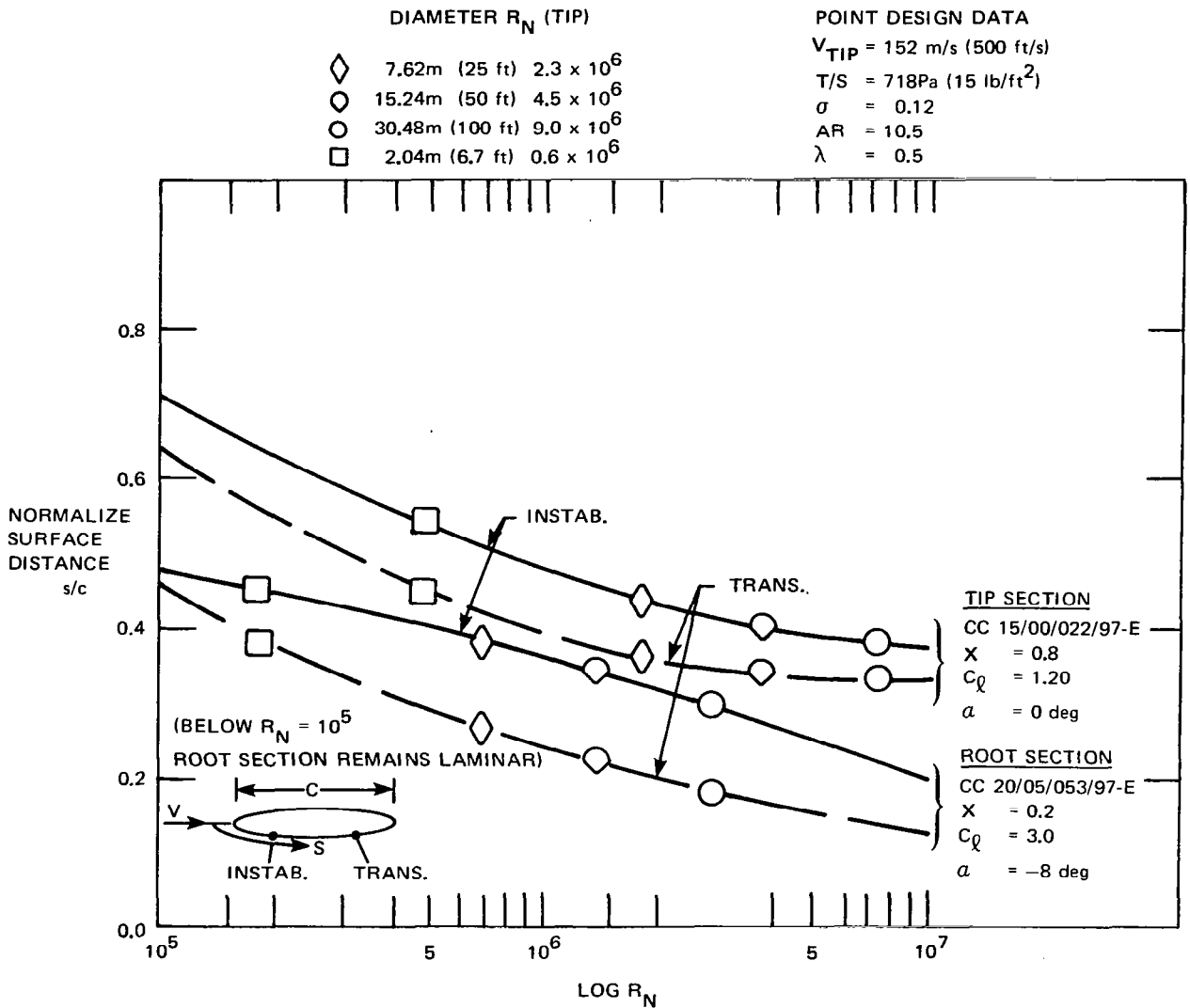


Figure 10.- Calculated instability and transition points for the X-Wing root and tip sections (demonstrating transition and hence avoidance of instability tone noise mechanism).

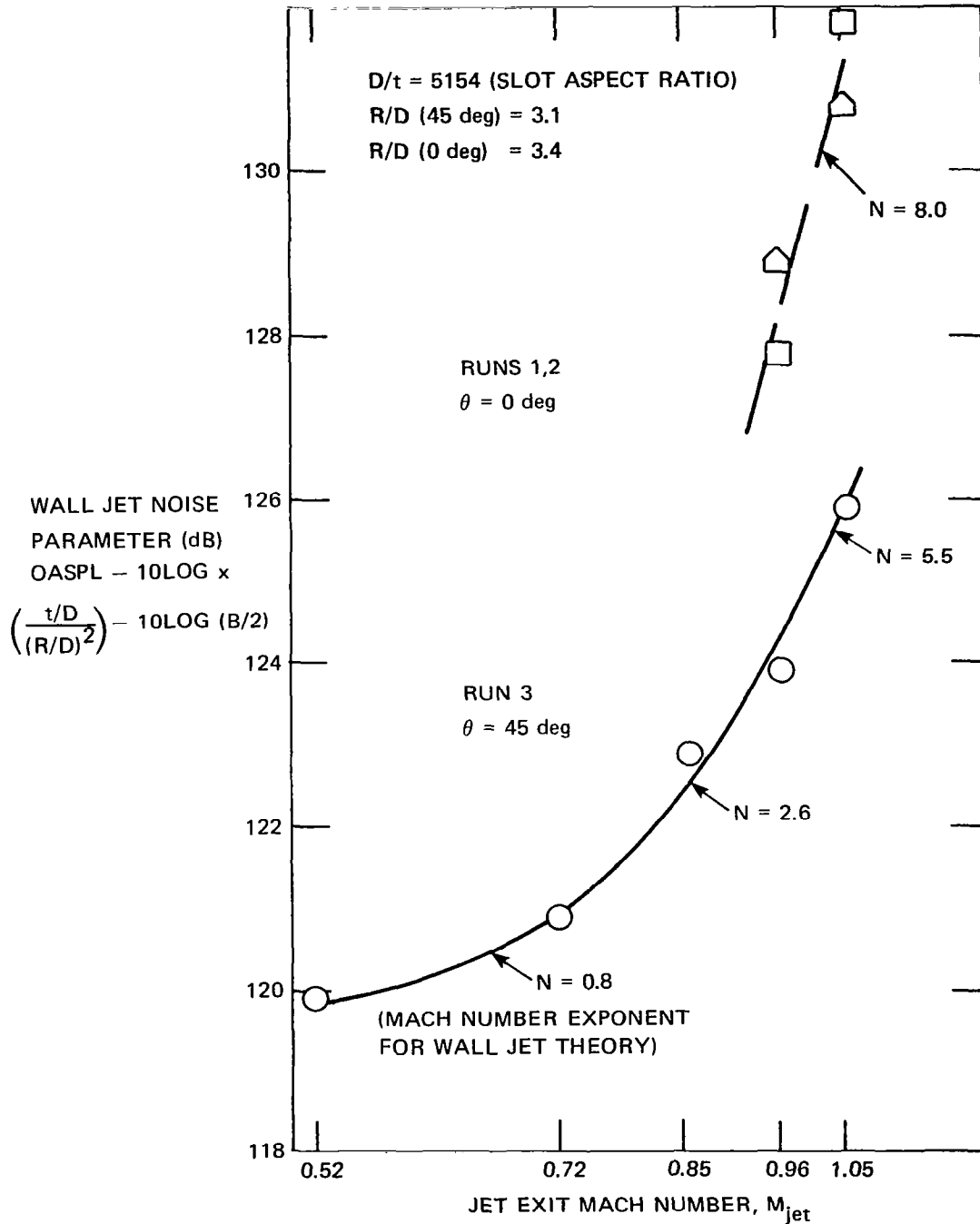


Figure 11.- Variation of measured Coanda 'jet noise' from NGTE 3.66 m (12 foot) CCR tests.

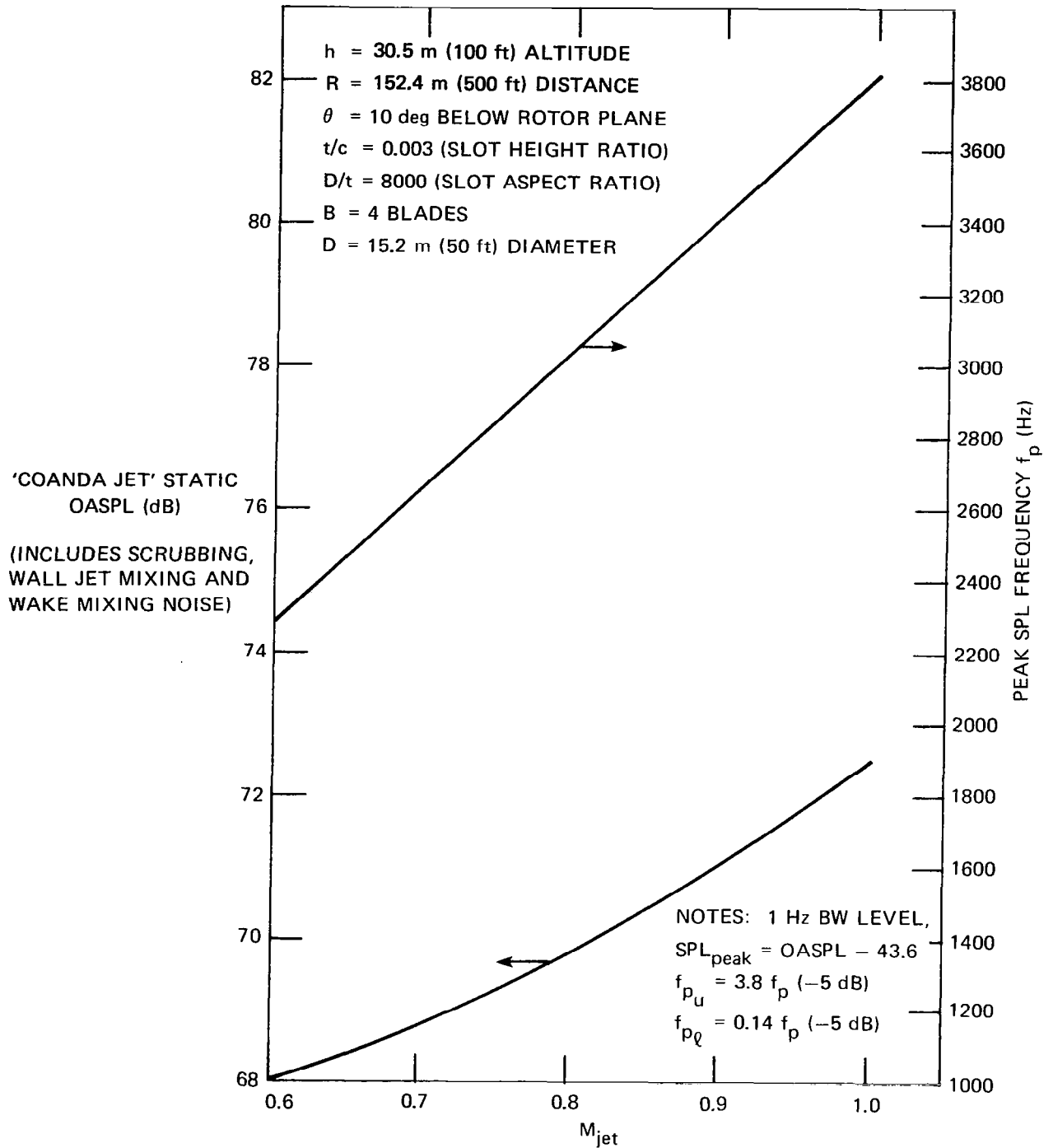


Figure 12.- Calculated 'Coanda jet' OASPL and frequency for a 15.2 m (50 foot) diameter (static rotor-worst case).

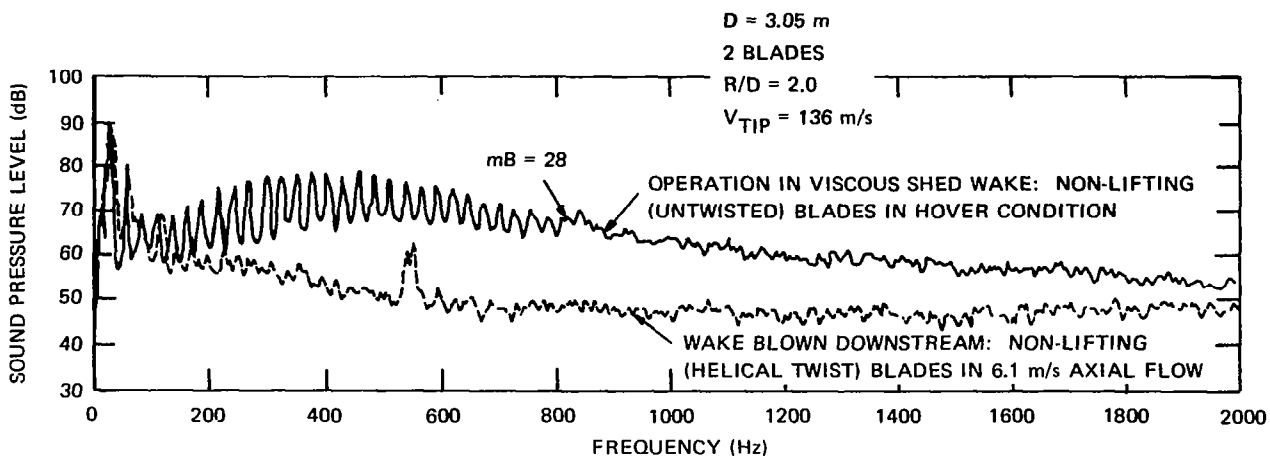


Figure 13.- Incident turbulence noise produced by two nonlifting NACA 0012 rotors (from ref. 9).

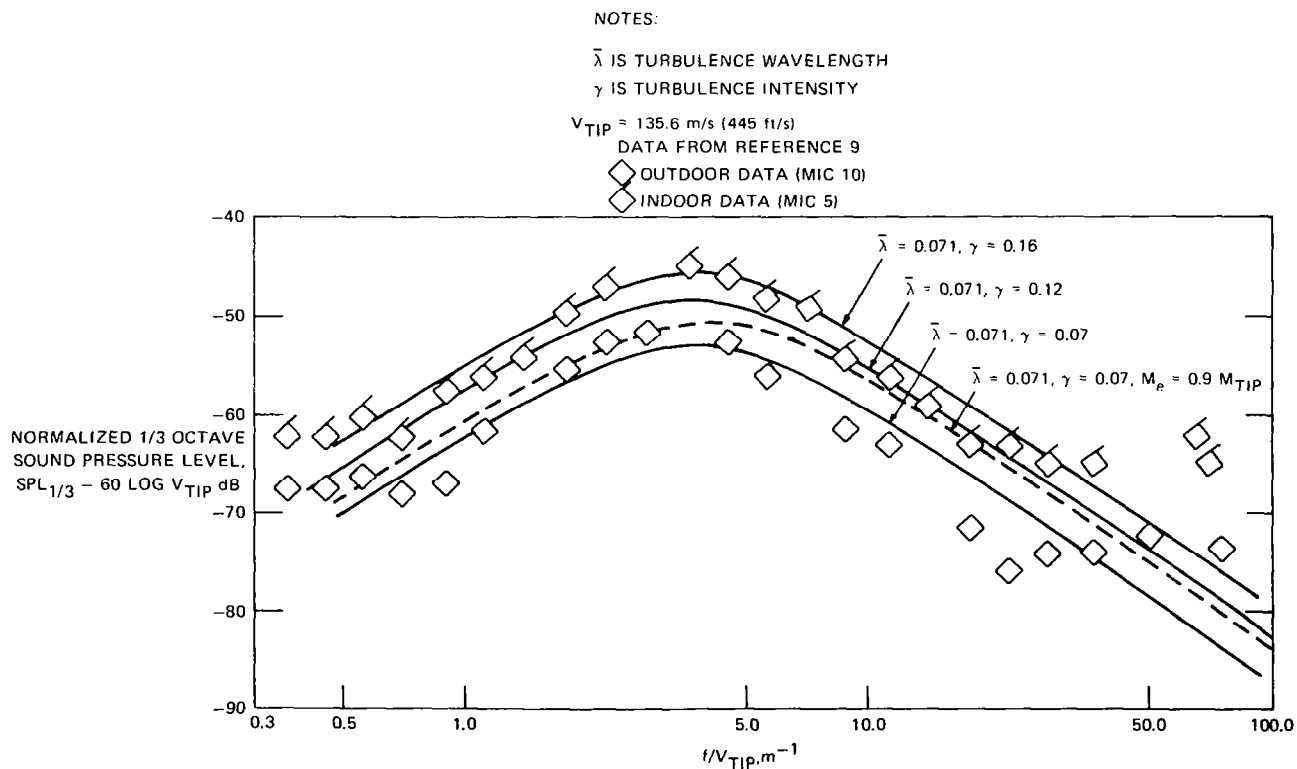
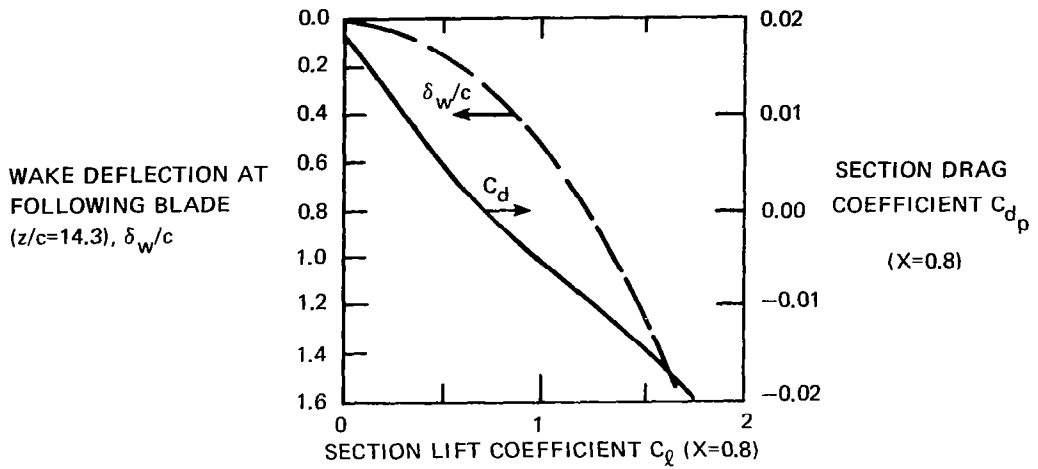
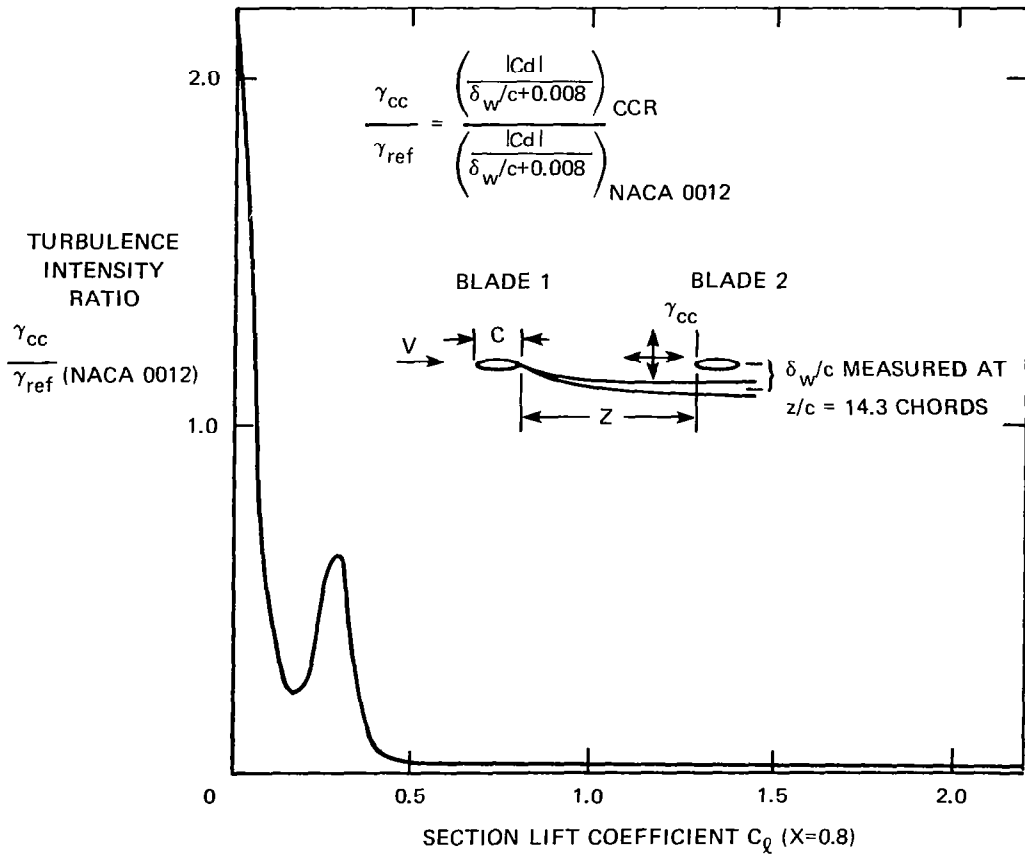


Figure 14.- Comparison of experimental incident turbulence data for an untwisted NACA 0012 rotor operating in its own viscous wake (zero lift) and incident turbulence theory modified from reference 10.

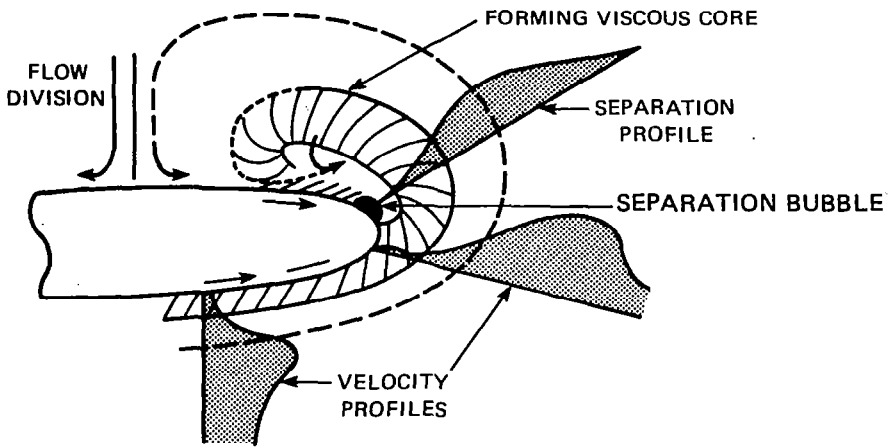


(a) Estimated wake deflection with lift variation.

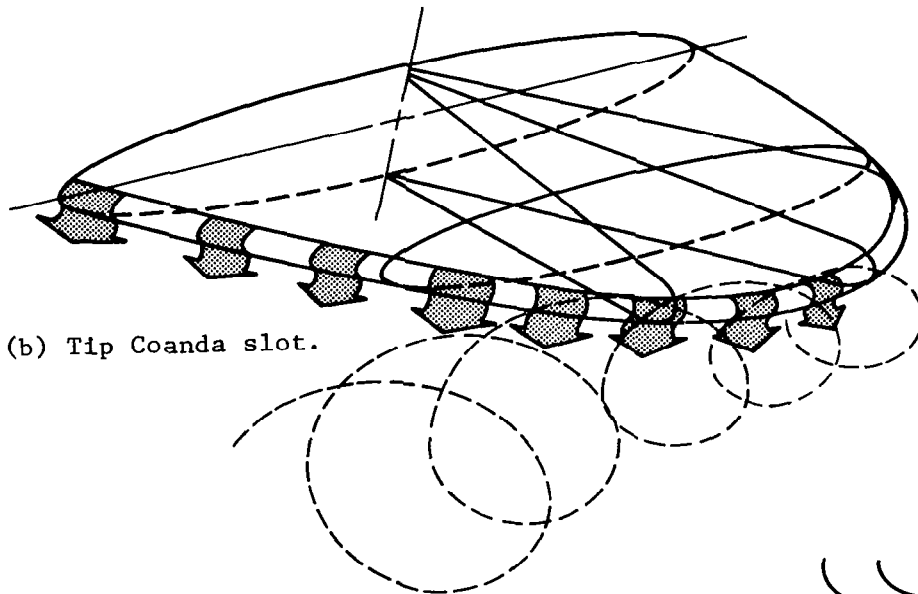


(b) Variation of turbulence intensity ratio with lift.

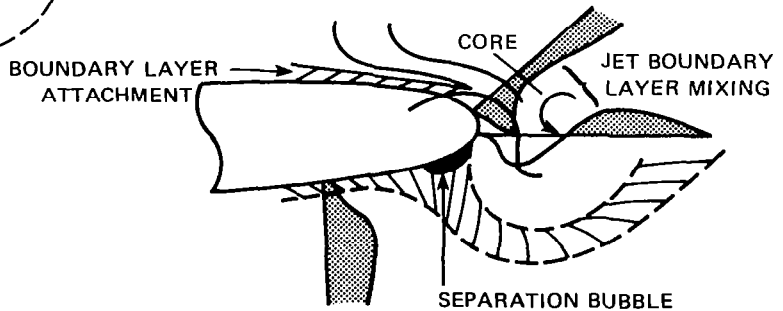
Figure 15.- Estimated viscous wake deflection and turbulence intensity of X-Wing tip section (relative to an untwisted NACA 0012 rotor operating in its own wake).



(a) No blowing - vortex core inboard.

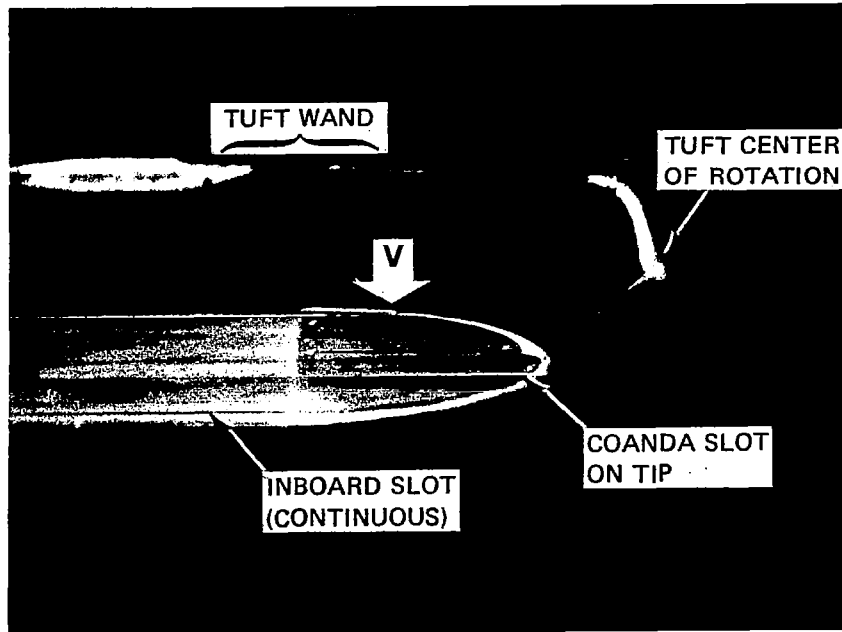


(b) Tip Coanda slot.

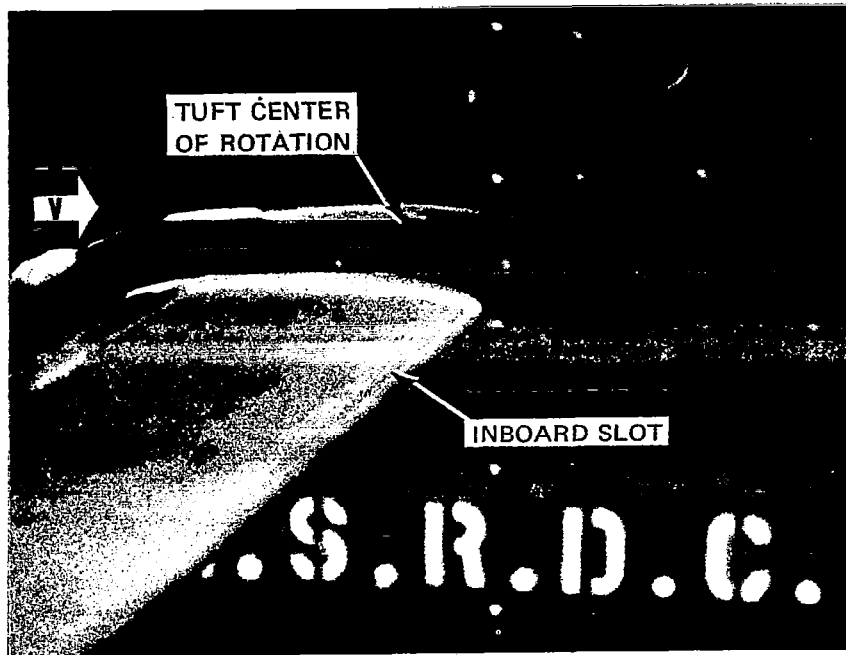


(c) Vortex core outboard.

Figure 16.- Conceptual function of Coanda tip blowing design.



(a) View from top and rear.



(b) View along span.

Figure 17.- Tuft wand flow studies of the effect of Coanda tip blowing on the formation of the vortex off the tip.

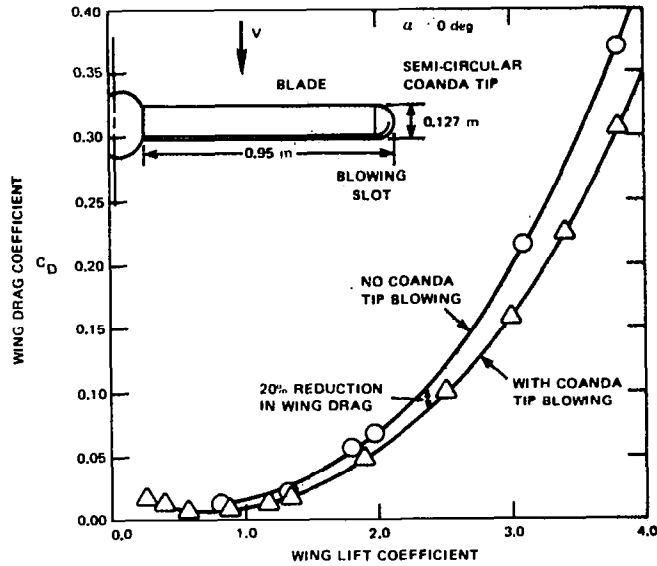


Figure 18.- Effect of Coanda tip blowing on drag of a single circulation control blade tested as a fixed wing.

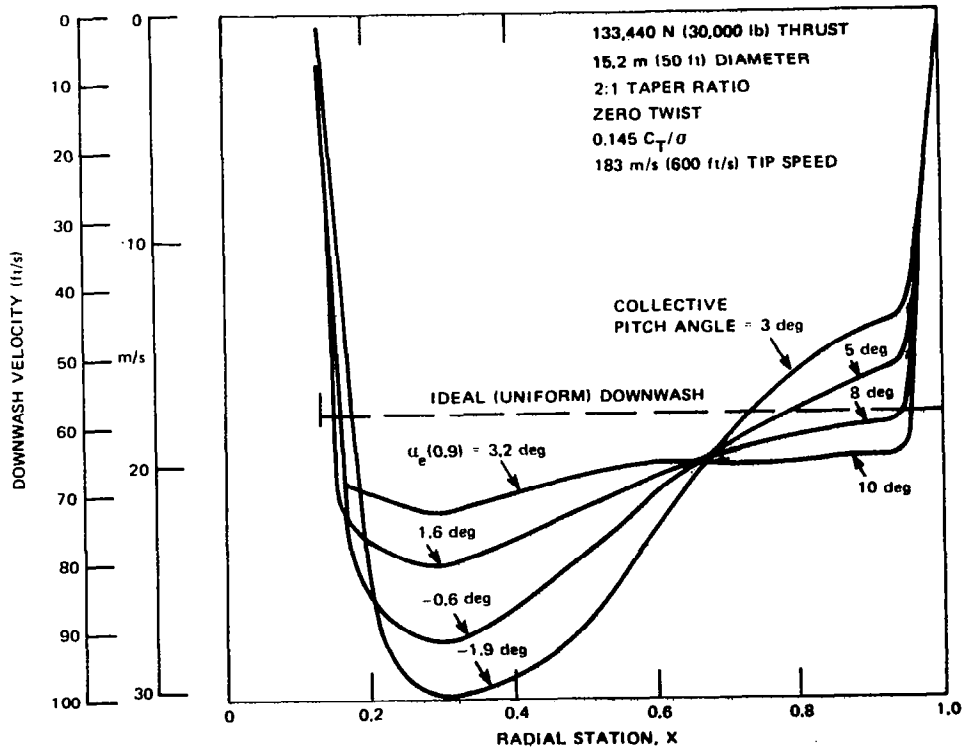


Figure 19.- Approximate induced velocity distribution of an X-Wing CCR in hover.

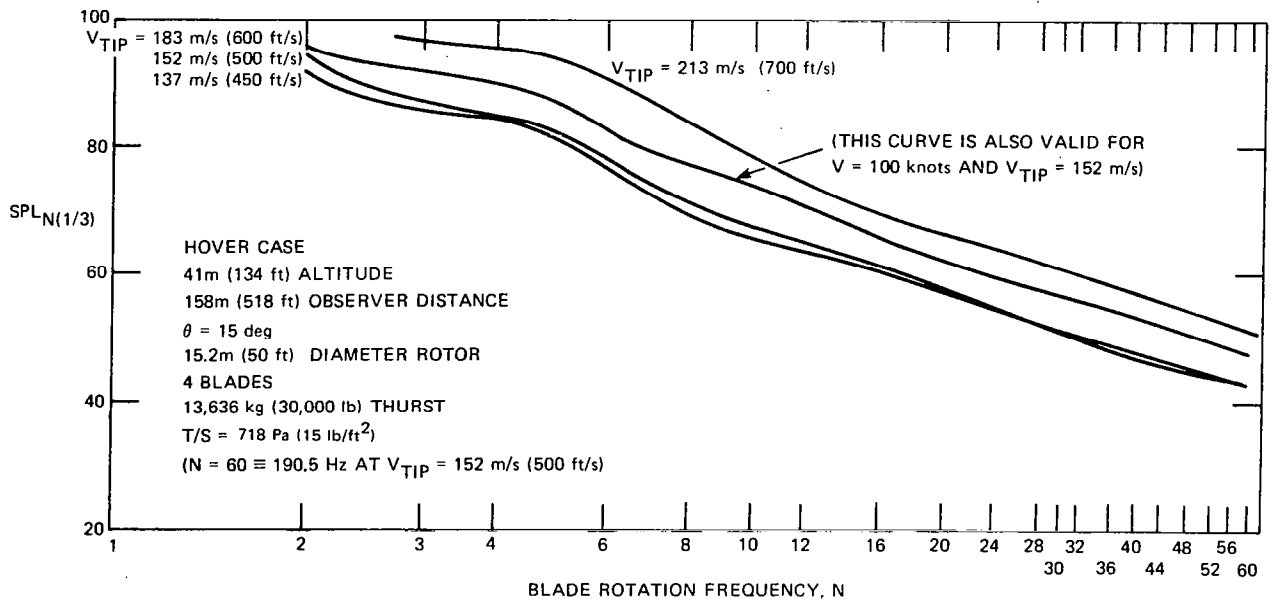


Figure 20.- Calculated effect of tip speed on rotational noise spectrum of 15.2 m (50 foot) diameter X-Wing.

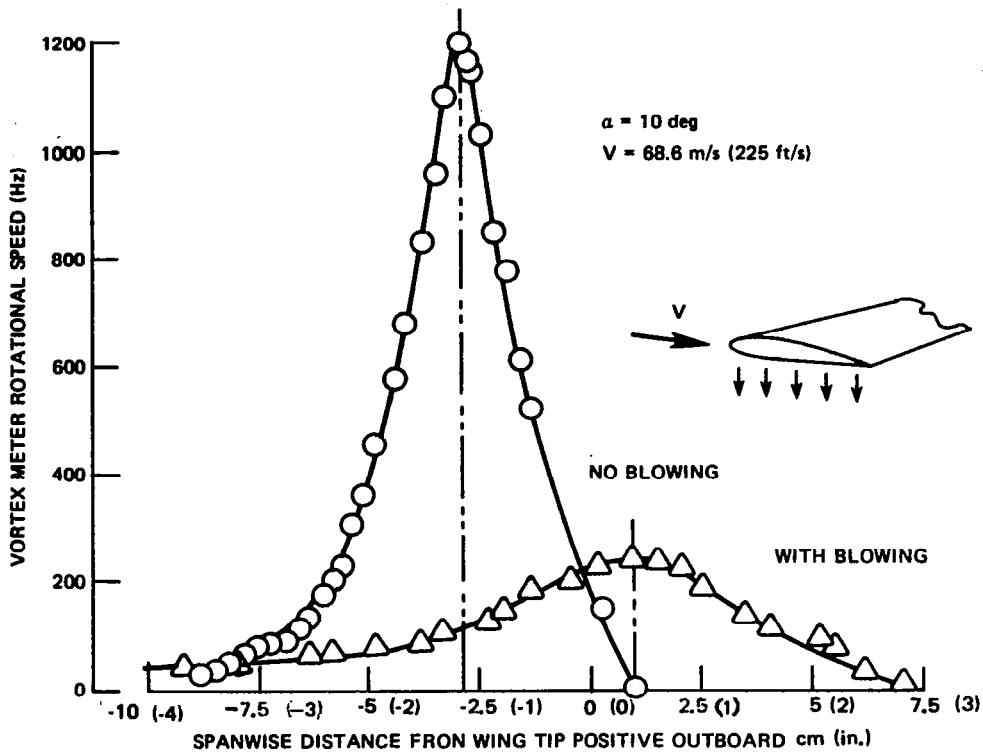


Figure 21.- Effect of normal chordwise blowing from reference 13 showing spanwise vorticity surveys with and without mass injection from nozzle #1v.

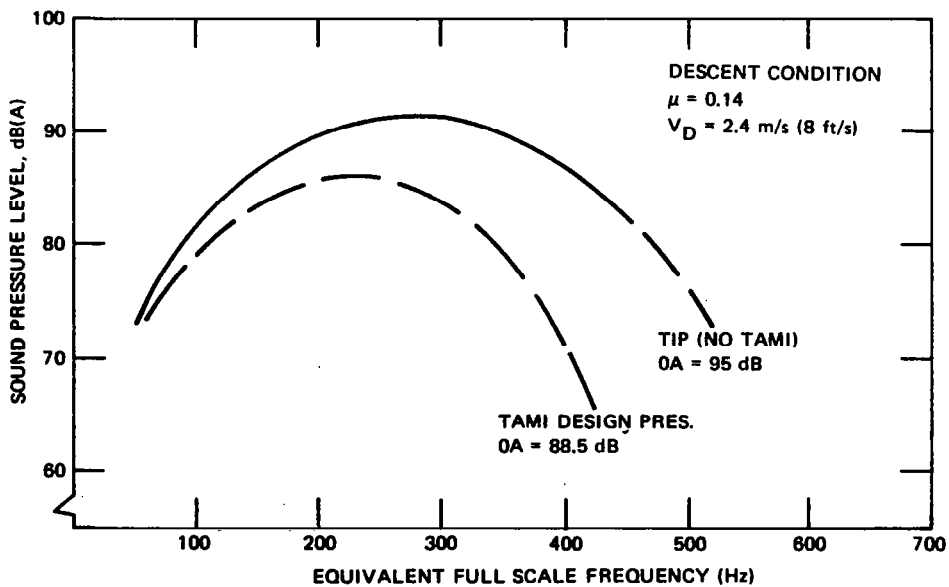


Figure 22.- Sound pressure level dB (A) with and without axial Tip Air Mass Injection (TAMI) into forming vortex core (from ref. 14).

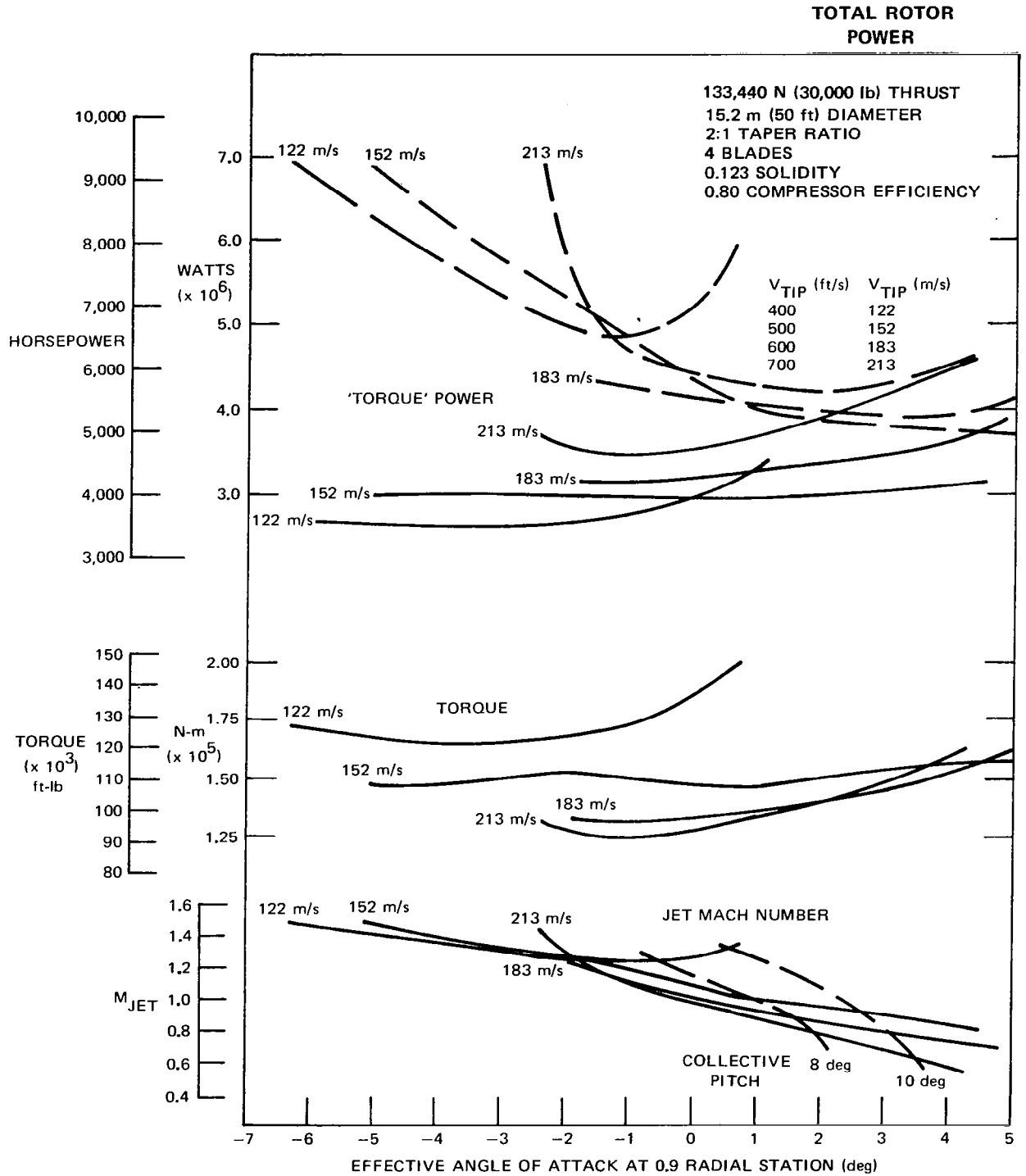


Figure 23.- Variation of X-Wing rotor hover performance parameters with angle of attack and tip speed.

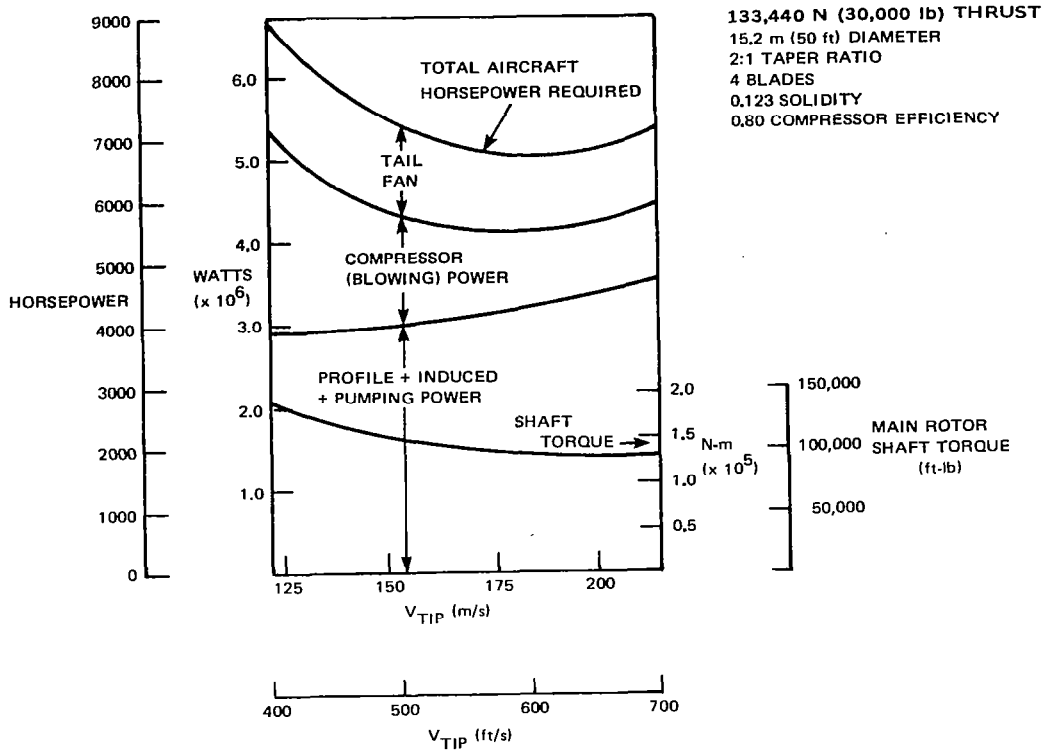


Figure 24.- Variation of power requirements in hover for an X-Wing VTOL (comparison performed for constant (zero) angle of attack at 0.90 radial station).

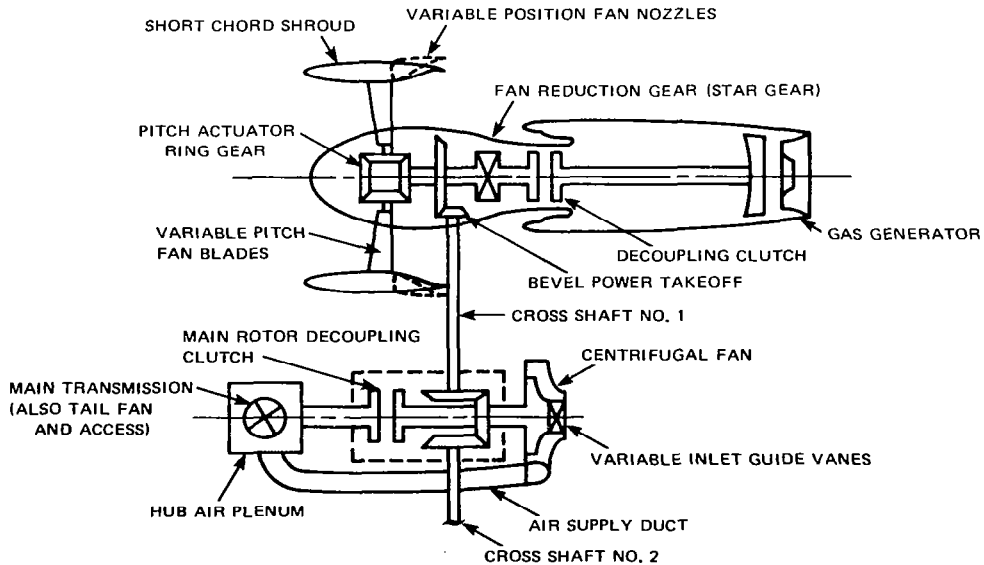


Figure 25.- One possible propulsion system arrangement for the X-Wing (twin, convertible, low noise, compound fan-shaft engines and centrifugal compressor).

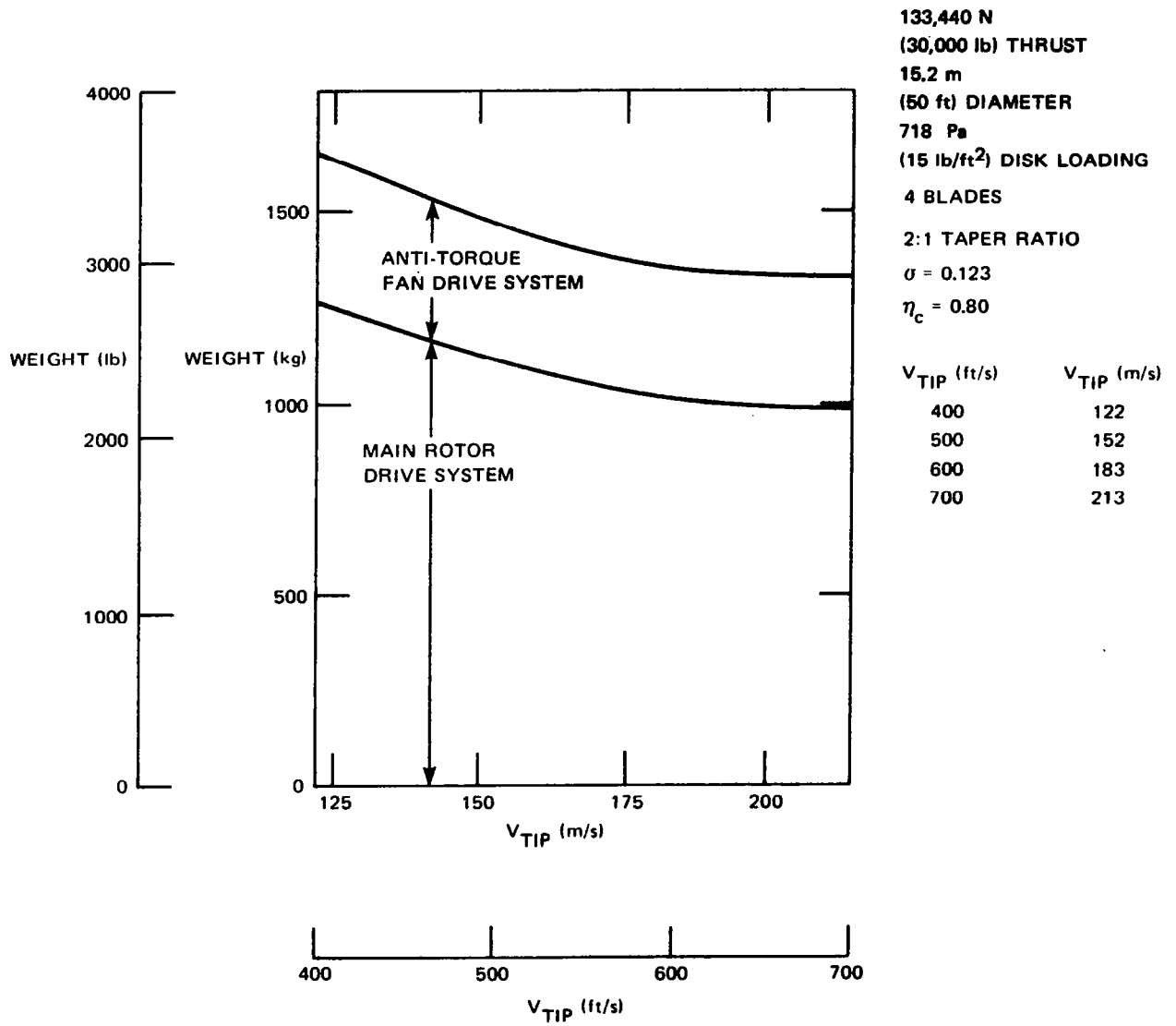


Figure 26.- Drive system and antitorque tail fan weight trends with tip speed.

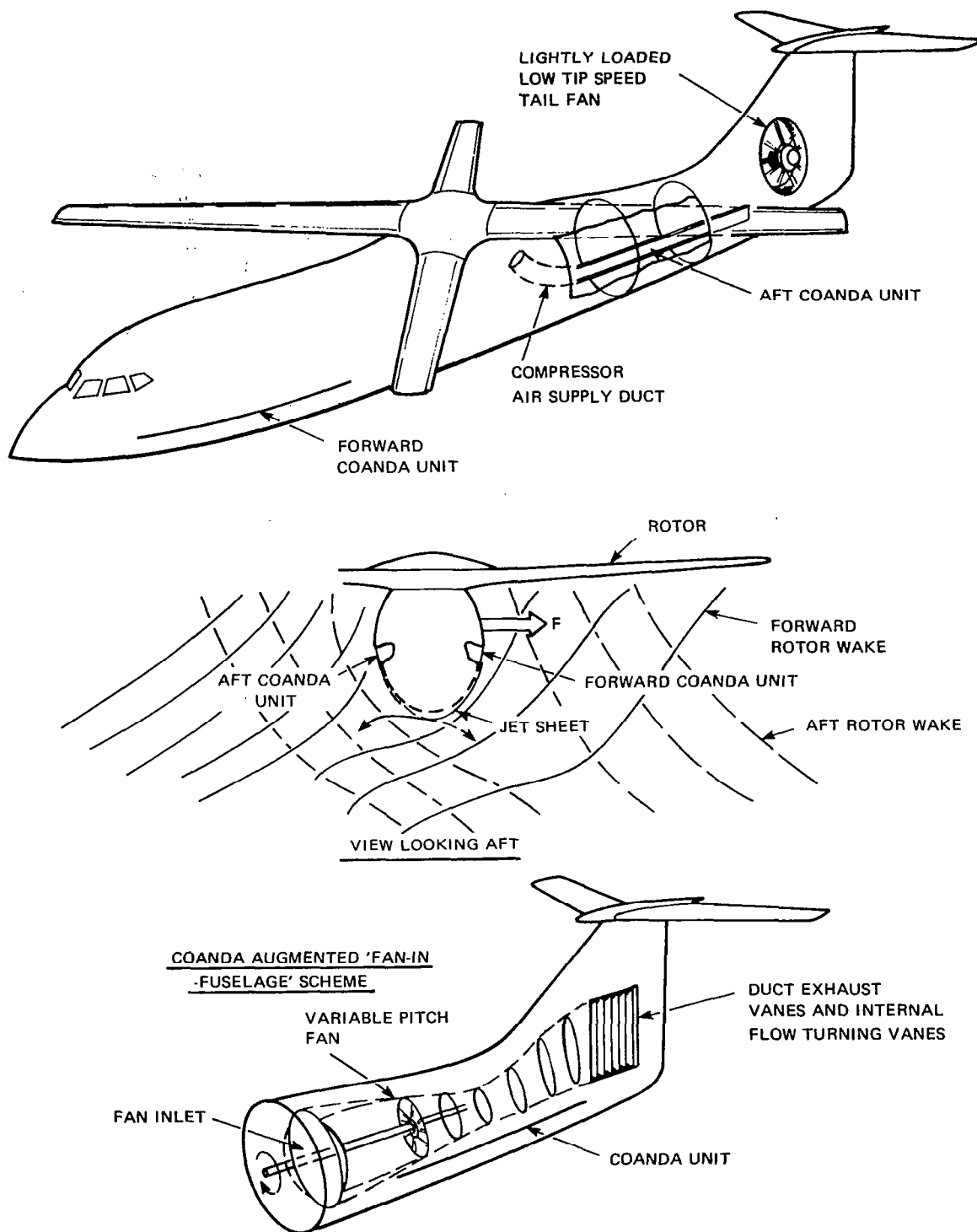


Figure 27.- Coanda blowing units to produce antitorque moments and low noise in hover and low speeds.